Title: What martian meteorites reveal about the interior and surface of Mars

Authors: Udry A.[1*], Howarth G. H.[2], Herd C. D. K.[3], Day J. M. D.[4], Lapen T. J.[5], and Filiberto J.[6]

Affiliations:
[1]Department of Geosciences, University of Nevada Las Vegas, 4505 S. Maryland Pkwy, Las Vegas, NV 890154
[2]Department of Geological Sciences, University of Cape Town, Rondebosch 7701, South Africa
[3]Department of Earth and Atmospheric Sciences, University of Alberta, Edmonton, AB, T6G 2E3
[4]Scripps Institution of Oceanography, University of California San Diego, La Jolla CA 92093
[5]Department of Earth and Atmospheric Sciences, University of Houston, Houston TX 77204
[6]Lunar and Planetary Institute, USRA, 3600 Bay Area Blvd., Houston, TX 77058, USA

*Corresponding author: Arya Udry (*arya.udry@unlv.edu)*

Word Count (Abstract 250, Text 13029)

Keywords
Martian meteorites, planetary processes, Mars 2020

Table of Contents

Abstract

Martian meteorites are our only samples from Mars, thus far. Currently, there are a total of 252 individual samples originating from ≥ 11 ejection sites with crystallization ages varying from 4.5 to 0.15 Ga. Analyses, through techniques that are also used on terrestrial rocks, allow fundamental insights into the bulk composition, differentiation and evolution, mantle heterogeneity, and role of secondary processes, such as aqueous alteration and shock, on Mars. Martian meteorites display a wide range in mineralogy and chemistry, but are predominantly basaltic in composition. Over the past six years, the number of martian meteorites recovered has almost doubled allowing for studies to evaluate these meteorites as suites of martian igneous rocks. However, the martian meteorites represent a biased sampling of the martian surface with unknown ejection locations. Thus, the geology of Mars cannot be unraveled solely by analyzing meteorites. Rocks measured by rovers at the surface are of distinct composition to the meteorites, highlighting the importance of Mars missions, especially sample return. The Mars 2020 *Perseverance* rover will collect and cache — for eventual return to Earth — over 30 diverse surface samples from Jezero crater. These returned samples will allow for Earth-based state-of-the-art analyses on diverse martian rocks with known field context. The complementary study of returned samples and meteorites will help constrain the evolution of the martian interior and surface. Here, we review recent finds and advances in the study of martian meteorites and provide a wish list of returned samples that would complement and enhance their study.

Plain-language summary

Scientists can learn about the formation and evolution of planets, such as Mars, by studying rock samples. Gaining rock samples from Mars allows for them to be studied in state-of-the-art laboratories on Earth with high precision and accuracy. Currently, samples are obtained from the surface of Mars through meteorites that have been ejected from the planet. We can study these rocks like we do rocks from Earth to learn about the volcanic processes, chemistry, and the timing of these events in martian geology. This review paper summarizes information we have learned about martian geology through analyzing its meteorites. Most of the data collected provides evidence that the interior of Mars is chemically varied with a high diversity in chemical makeup throughout time. However, most meteorites are relatively young with few older rocks (≥ 2.4 billion years old) analyzed to date. Fortunately, the Mars 2020 mission will return samples directly from Mars's surface: These samples will be collected from the Jezero crater and will be brought back to Earth as early as 2031. The study of both meteorites and returned samples is essential to study representative rocks from Mars as well as rocks originating from different locations on the Red Planet.

1. Introduction

For the past 55 years, orbiters have documented the global mineralogy, composition, and geomorphology of Mars. Landers and rovers have constrained field context and measured the chemistry and mineralogy of surface rocks *in situ,* including remote and contact analyses. However, instruments deployed on the martian surface by landers and rovers do not have the precision and accuracy of analytical techniques employed in Earth-based laboratories, cannot examine multiple physical or geochemical sample parameters, nor can they reproduce the field context provided by human beings. Analyses in terrestrial laboratories can determine the chemistry, mineralogy, elemental and isotopic compositions, as well as physical properties of samples from hand-sample to the atomic scale. Using samples, several fundamental planetary

processes have been documented. These include the timing and nature of emplacement and formation of magmatic rocks, the nature and timing of planetary accretion and differentiation, the chemical and isotopic diversity of the mantle, the distribution and evolution of volatile compounds in and on Mars, environments and timing of alteration and weathering, and impact processes (Figure 1).

Certain classes of martian meteorites are the only samples currently available from Mars. Crater-forming meteorite impact events on Mars generated sufficient energy to eject fragments of the crust through the atmosphere and into space (escape velocity ~5 km/s; Fritz et al., 2005) through near-surface spallation (e.g., Head et al., 2002). Fragments of these ejection events represent the martian meteorites that have so far been recovered in Antarctica, Northwest Africa, Chile, USA, India, Nigeria, Mali, Mauritania, Brazil, and Oman.

Martian meteorites were traditionally divided into three main groups: called the shergottites, nakhlites, and chassignites, after their namesake meteorites, Shergotty, Nakhla, and Chassigny. As such, igneous protolith (herein referred to as simply igneous) martian meteorites are also referred to as 'SNCs'. The traditional 'SNCs' have mafic to ultramafic compositions (~4 to 30 wt.% MgO). In addition, martian meteorites include a few specimens that do not fall into the traditional 'SNC' classification: the orthopyroxenite Allan Hills (ALH) 84001 and the polymict breccia NWA 7034 and its 16 paired meteorites. Most martian meteorites are geologically young (Amazonian), with shergottites predominantly being mid- to late-Amazonian in age (<716 Ma), with only two examples (NWA 7635 and NWA 8159) having a 2.4 Ga early Amazonian ages, and nakhlites and chassignites are dated at ~1.3 Ga (Borg et al., 2002, 2003; Brennecka et al., 2014; Cohen et al., 2017; Herd et al., 2017; Lapen et al., 2017; Nyquist et al., 2001, 2009; Righter et al., 2018). There are two Noachian lithologies: ALH 84001 dated at 4.1 Ga, and igneous clasts within NWA 7034 that are as old as 4.5 Ga (Bellucci et al., 2018; Bouvier et al., 2018; Lapen et al., 2010; McCubbin et al., 2016).

Stolper & McSween (1979) and McSween & Stolper (1980) first proposed that the meteorites Shergotty and Zagami were derived from Mars: their chemistry, mineralogy, and ages suggested that they originate from a body large enough to still be volcanically active during the last half billion years. The first definitive evidence for a martian origin was accomplished by linking the martian atmospheric noble gases, C, and N isotopic compositions and concentrations measured by the Viking landers in 1976 to trapped gas compositions in impact-melt glasses in the Elephant Moraine (EETA) 79001 meteorite (Bogard & Johnson, 1983). While such studies have only been completed for a handful of these meteorites, all suspected martian meteorites are now confirmed using their bulk oxygen isotopic compositions. Mars has $\Delta^{17}O$ isotopic compositions that are ~0.3‰ heavier than terrestrial or lunar samples and fall along a mass-dependent fractionation line (e.g., Ali et al., 2016). Although the exact location of origin for meteorites on the martian surface is currently unconstrained, the mineralogy, petrology, major and trace element and isotopic compositions, and ages of martian meteorites have been fundamental for providing constraints on the evolution of the red planet throughout its geologic history.

The Mars 2020 rover *Perseverance* is the first mission in a series that will eventually cache over 30 samples from Jezero crater, for return to Earth as early as 2031 (IMOST, 2018). For the first time, we may have access to samples with a known field context and location at the martian surface. In addition to the ability for analysis in Earth-based laboratories, these returned samples will presumably represent the geologic diversity for one location. They will also provide opportunity for ground truth of remote-sensing analyses and help to calibrate crater age counting on Mars if ages on the collected rocks can be obtained and their stratigraphic relationships constrained. Here we provide a review of the main discoveries from martian meteorites, paying particular attention to the latest discoveries in the last six

years, their significance for understanding martian geology, and the implications of their study for the suite of desired returned samples from Jezero crater.

2. A variety of lithologies representing predominantly igneous martian processes

2.1. Source and availability of martian meteorites

At the time of publication of this manuscript, 252 officially classified martian meteorites have been recovered, suggested to represent 141 pairing groups. Paired meteorites originate from the same parent meteoroid that broke up into several pieces upon ejection from Mars or upon entry into Earth's atmosphere. Table S1 is a compilation of the entire list of martian meteorites, including paired groups. Note that not all paired groups have been confirmed in peer-reviewed publications and are based on the meteorite list created by A. J. Irving (https://imca.cc/mars/martian-meteorites-list.htm). Table S2 includes the number of meteorites per type, for paired groups and unpaired individual meteorites. The total mass of martian meteorites is ~198 kg, with the most massive meteorites, including recovered strewn field stones, being Zagami (~18 kg), Tissint (~12 kg), and Nakhla (~9.9 kg).

The rate of recovery of martian meteorites has varied significantly over the last two centuries (Figure 2). Five witnessed meteorite falls have been reported, including: the first discovered martian meteorite Chassigny in 1815 (Champagne-Ardenne, France), Shergotty in 1865 (Bihar, India), Nakhla in 1911 (Al Buhayrath in Egypt), Zagami in 1962 (Katsina, Nigeria), and Tissint in 2011 (Guelmim-Es-Semara, Morocco). A total of 30 samples have been recovered in Antarctica by the US Antarctic Search for Meteorites (ANSMET) and Japanese National Institute of Polar Research (NIPR) missions. The numbers of martian meteorites have increased dramatically since the first discovery, with nine by 1980, 25 by 2000, and 57 by 2010 (Fig. 2). Since 2014, 64 martian meteorites have been recovered, constituting 45% of the current collection, all of them found in Northwest Africa, Oman, and Chile (Fig. 2). They include 60 shergottites, three nakhlites, and one chassignite. This increase in recovery rate is due to the fact that meteorite hunters, especially in Northwest Africa, have become extremely efficient at identifying valuable achondrites, helped in part by increased access to online resources and social networking, as well as a better understanding of the scientific and financial value of martian meteorites (Mendy Ouzillou, personal communication).

2.2. The different types of martian meteorites

With the exception of the polymict breccia lithologies, all other martian meteorites recognized to date have igneous origins. In general terms, these igneous rocks range in composition from mafic to ultramafic and generally contain variable proportions of augite, pigeonite, maskelynite (plagioclase that has been shock metamorphosed to a diaplectic glass in most specimens), olivine, and orthopyroxene, and minor minerals including Cr-spinel, phosphates (merrillite, apatite), sulfides, titanomagnetite, ilmenite, ± baddeleyite and ± silica. The textures of the different groups of martian meteorites are aphanitic, porphyritic, diabasic (= microgabbroic), and oikocrystic and are described below in this section (also represented in figure 3).

Over the past several years, a large diversity in lithologies, textures, chemistries, igneous crystallization ages, and initial radiogenic isotopic compositions have been observed for martian meteorites, especially for shergottites. In this section, we describe the diversity among meteorites from Mars. Different groups of martian meteorites are distinguished based on their trace element geochemistry and radiogenic isotopic compositions (yielding insights

on the mantle sources), emplacement histories (known by mineralogy and textures), and crystallization and ejection ages (based on measurements of long-lived and short-lived isotopic systems). A compilation of all published martian meteorite bulk compositions is provided in Table S3. This table also includes igneous compositions found at Gusev and Gale craters. Other compilations of bulk major element data are also found in Filiberto (2017) and Treiman and Filiberto (2014).

2.2.1. Shergottites

The shergottites are the most abundant type of martian meteorites, accounting for 83% of the total collection by number and 80% by mass. Shergottites are geochemically classified based on their relative enrichment or depletion in incompatible trace elements (ITE) and these ITE compositions are largely inherited from their mantle sources. The large predicted range in ITE compositions of the martian mantle likely formed during silicate planetary differentiation and crystallization after a magma ocean phase (e.g., Borg and Draper, 2003; Debaille et al., 2008) very early in Mars history (e.g., Debaille et al., 2007; Borg et al., 2016). The long-term variations in mantle ITE compositions have resulted in relatively large variations in radiogenic isotopic compositions in these mantle sources. During partial melting of these mantle sources, their isotopic compositions have been imparted into the shergottites derived from them (e.g., Borg et al., 2003; Lapen et al., 2017). Thus, coupled variations in ITE and radiogenic isotopic compositions are used to distinguish three groupings of shergottites (Figure 4). These groups include specimens that are either relatively enriched in ITE, depleted in ITE, or have compositions intermediate between the enriched and depleted groupings. Depleted shergottites have bulk rock rare earth elements (REE) compositions with $(La/Yb)_{CI}$ <0.3 and have relatively low initial $^{87}Sr/^{86}Sr$, $^{207,206,208}Pb/^{204}Pb$, and $^{187}Os/^{188}Os$ ratios, and relatively high initial $^{142,143}Nd/^{144}Nd$ and $^{176}Hf/^{177}Hf$ ratios. Enriched shergottites have REE compositions relatively enriched in the more incompatible REE resulting in $(La/Yb)_{CI} > 0.8$. The relative enrichment in ITE is associated with relatively high initial $^{87}Sr/^{86}Sr$, $^{207,206,208}Pb/^{204}Pb$, and $^{187}Os/^{188}Os$ ratios, and relatively low initial $^{142,143}Nd/^{144}Nd$ and $^{176}Hf/^{177}Hf$ ratios. Intermediate shergottites, with $(La/Yb)_{CI}$ of 0.3 to 0.8, represent compositions intermediate between the enriched and depleted endmember compositions (Armytage et al., 2018; Borg et al., 2003; Borg et al., 2016; Borg et al., 2002; Brandon et al., 2012; Brennecka et al., 2014; Combs et al., 2019; Debaille et al., 2008; Ferdous et al., 2017; Filiberto et al., 2012; Lapen et al., 2017; McSween, 2015; Nyquist et al., 2001; Shafer et al., 2010; Symes et al., 2008; Tait & Day, 2018; Usui et al., 2010). Shergottite sources are further described in section 4.1.

Shergottites can be classified into different groups according to their texture (i.e., grain size, shapes, and modal abundances). The different textures represent mineral formation and emplacement in the shallow subsurface or perhaps erupted at the surface. First are the basaltic shergottites, which mostly contain pyroxene (average lengths of 0.3 mm, up to 1 mm) and maskelynite and are characterized by the absence of olivine phenocrysts or megacrysts (e.g., He et al., 2015; Howarth et al., 2018; McSween et al., 1996; Rubin et al., 2000). Second in abundance are the olivine-phyric shergottites, which are porphyritic and contain olivine phenocrysts (sometimes megacrystic with sizes up to 2.5 mm) with later-crystallizing olivine, pyroxene, and maskelynite (grains in the groundmass of ~0.25 mm; e.g., Balta et al., 2015; Basu Sarbadhikari et al., 2016; Chen et al., 2015; Dunham et al., 2019; Goodrich, 2002; Liu et al., 2016). Third are the poikilitic shergottites that contain olivine chadacrysts (up to 1.8 mm) enclosed by large pyroxene oikocrysts (from 3 to 10 mm in length), with later-crystallizing olivine, pyroxene, and maskelynite (Combs et al., 2019; Howarth et al., 2014; Kizovski et al., 2019; Rahib et al., 2019; Walton et al., 2012). Poikilitic shergottites were previously termed

lherzolitic shergottites (e.g., Mikouchi & Kurihara, 2008). However, in the last decade, numerous new finds and descriptions of this group of shergottites has shown that many of them have >10% plagioclase, and thus, are not lherzolites *sensu stricto* (Walton et al., 2012). The fourth type are gabbroic shergottites, which contain cumulate pyroxene or plagioclase (Filiberto et al., 2018; Filiberto et al., 2014; Udry et al., 2017). Most shergottites studied before 2014 were fine-grained or diabasic, but new gabbroic specimens (= crystallized at depth under the martian surface) have now been recovered, including NWA 6963 (pyroxene cumulate) and NWA 7320 (plagioclase cumulate) (Udry et al., 2017, Filiberto et al., 2018, Hewins et al., 2019). Gabbroic shergottites are similar to basaltic shergottites but have a cumulate texture (with average grain size of cumulus grains of pyroxene or plagioclase > 1 mm up to 5 mm in length) and geochemically show indications of crystal accumulation. They may be related to basaltic shergottites through magmatic processes (see section 3.1.). Hewins et al. (2019) describe NWA 10414, which is a pigeonite-rich (73 mod.%) cumulate shergottite, with pigeonite grain lengths up to 4 mm. It is a distinctive shergottite, as it does not contain augite in any significant quantity. A recent discovery among the olivine-phyric shergottites is the presence of olivine phenocrysts that display concentric core-to-rim color differences in transmitted light, from amber to red-brown to clear (e.g., NWA 7042, Izawa et al., 2015; NWA 10416, Piercy et al., 2020; Vaci et al., 2020). While the alteration of olivine to iddingsite is not uncommon in the martian meteorites (attributable to either low-temperature aqueous alteration on Mars or a similar process on Earth), this particular texture is distinct, and has been suggested to be due to deuteric alteration (i.e., reaction with magmatic fluids during crystallization (Kuebler, 2013; Vaci et al., 2020) or, alternatively, preferential terrestrial alteration (Piercy et al., 2020).

Two recently described shergottites, NWA 7635 and NWA 8159, are distinct in texture and crystallization age from the other shergottites, but which overlap in ejection age (see section 5). Northwest Africa 7635, dated at 2.40 ± 0.14 Ga, consists of phenocrysts of maskelynite (up to 200 μm in length), augite, and olivine in a maskelynite and pyroxene groundmass, but lacks pigeonite (Lapen et al. 2017). Northwest Africa 8159, dated at 2.37 ± 0.25 Ga, has an intergranular texture of plagioclase (partially converted to maskelynite), augite, and olivine (with grain sizes varying from 100 to 200 μm), and also lacks pigeonite. Low-Ca pyroxene in this rock is the result of a subsolidus reaction (Herd et al. 2017). Both rocks are depleted in LREE with $(La/Yb)_{CI}$ ~0.1, but with a slightly different Dy/Lu ~ 0.84 (compared to Dy/Lu > 1 in other shergottites). Nevertheless, the depleted nature, geochemistry, and radiogenic isotopic characteristics of NWA 7635 suggest that it is derived from the same mantle sources as the depleted shergottites (Lapen et al., 2017).

The majority of the shergottites are late Amazonian in age with enriched shergottite crystallization ages ranging from 165 to 225 Ma (Borg et al., 2008; Combs et al., 2019; Ferdous et al., 2017; Lapen et al., 2009; Moser et al., 2013; Nyquist et al., 2001; Shafer et al., 2010; Usui et al., 2010), intermediate shergottites ranging from 150 to 346 Ma (Borg et al., 2002; Nyquist et al., 2001, 2009) and depleted shergottite ages from 327 Ma to 2.4 Ga (including NWA 7635 and 8159; Brennecka et al., 2014; Herd et al., 2017; Lapen et al., 2017; Nyquist et al., 2001; Shih et al., 2011). The timing of formation of shergottites and other meteorites is represented in figure 5. Using Pb-Pb isotopic compositions, Bouvier et al. (2008, 2009) proposed >4 Ga Noachian ages for all shergottites. However, other isotopic systems, such as Rb-Sr, Lu-Hf, Sm-Nd, U-Pb, and Re-Os, are concordant and yield Amazonian ages. Bellucci et al. (2015) proposed that the Pb-Pb compositions of shergottites do not represent an >4 Ga isochron age, but minor additions from an additional highly radiogenic, probably crustal reservoirs on Mars. The radiogenic Pb component may be widespread and mixed into virtually every martian meteorite (Bellucci et al., 2016; Gaffney et al., 2011). The combined

evidence from independent isotopic systems (Ar-Ar, Rb-Sr, Lu-Hf, Sm-Nd, Re-Os, and U-Pb) is that the shergottites have relatively young eruption ages, between 150 and 2400 Ma.

2.2.2. Nakhlites and chassignites

Nakhlites and chassignites make up ~10% of the total martian meteorite collection by number and 13% by mass. Nakhlites are ~1.3 Ga clinopyroxene-rich igneous rocks containing cumulus pyroxene and olivine (average lengths between 0.3 – 0.4 mm), with minor glass, plagioclase, phosphate minerals, fayalite-rich olivine in the mesostasis, titanomagnetite, and sulfide minerals. Chassignites are ~1.3 Ga dunitic rocks comprised of cumulus olivine (average 0.6 mm in length) with chromite inclusions and interstitial plagioclase, orthopyroxene, and phosphate minerals. All nakhlites and chassignites have similar crystallization (~1.3 Ga) and ejection (~11 Ma) ages (Cohen et al., 2017; Nyquist et al., 2001; Udry & Day, 2018). The similar ejection ages show that they all likely originate from the same location on Mars. Nakhlites and chassignites have the same depleted radiogenic isotopic compositions, with high $^{142}Nd/^{144}Nd$, and $^{182}W/^{184}W$, and low $^{87}Sr/^{86}Sr$, but these compositions are distinct from shergottites (Carlson & Boyet, 2009; Caro et al., 2008; Debaille et al., 2009; Foley et al., 2005; Nyquist et al., 2001). Although the nakhlites and chassignites were previously suggested to be unrelated (Wadhwa & Crozaz, 1995), their compositions, textures, and volatile-bearing minerals suggest they may originate from the same volcanic system (McCubbin et al., 2013; Udry & Day, 2018). Previous studies concluded that the nakhlites were emplaced as one magmatic body, often called a 'cumulate pile' (Berkley et al., 1980; Day et al., 2006; Mikouchi et al., 2012). The recovery and study of new nakhlites and chassignites since 2014 (Balta et al., 2017; Jambon et al., 2010; Tomkinson et al., 2015; Udry & Day, 2018), however, shows greater variation in mineralogy and composition compared to the previously observed samples, suggesting that these rocks were emplaced as several shallow sills and/or lava flows, and may not represent a singular magmatic body. Textural evidence also suggest that the nakhlites have undergone different emplacement and/or shock histories (Griffin et al., 2019; Udry & Day, 2018).

2.2.3 Allan Hills 84001

Allan Hills 84001 is an igneous cumulate orthopyroxenite (with grain size up to 3.5 mm) that contains minor chromite, augite, glass, olivine, apatite, and 1 vol.% of secondary phases including Fe-Mn-Mg carbonate, the latter notably containing magnetite inclusions and organic matter (Bradley, 1996; McKay et al., 1996; Mittlefehldt, 1994). Allan Hills 84001 underwent four to five shock events before being ejected from Mars 14.2 Ma (Eugster et al., 2002; Treiman, 1998). The igneous crystallization age is 4.09 ± 0.03 Ga (Lapen et al., 2010), with younger carbonates dated at 3.95 Ga (Borg et al., 1999; Beard et al., 2013). This meteorite became famous after McKay et al. (1996) declared that ALH 84001 showed evidence of past life on Mars, due to the presence of possible indigenous organic molecules (polycyclic aromatic hydrocarbons) and putative fossil bacteria, and because the magnetite inclusions in carbonate globules show chemical and physical characteristics similar to magnetite formed by magnetobacteria on Earth (Thomas-Keprta et al., 2000). However, several studies demonstrate that these features are likely to be abiotic (Anders et al., 1996; Treiman, 2019). A recent study by Koike et al. (2020) presents evidence for ancient N-bearing organic compounds preserved in secondary carbonate in ALH 84001. These authors hypothesize that the surface environments on Mars at the time of carbonate formation might have been less oxidizing than they are now. Carbonates were likely formed through neutral water at ~25 °C (Halevy et al., 2011; Valley et al., 1997). The Sr isotopic compositions of

carbonate indicate that the Sr contained in them was largely derived from phyllosilicates produced during pre-4.2 Ga low-temperature aqueous alteration of crustal rocks (Beard et al., 2013). Magnetite formed through shock metamorphism from the Fe-carbonates during rapid temperature increase along carbonate grain faces and edges (Treiman, 2003). In spite of the lack of convincing evidence for ancient life in this rock, the conditions recorded by the carbonates are suggestive of a habitable environment during the Noachian (Treiman, 2019).

2.2.4. Polymict regolith breccia NWA 7034 and its pairs

The polymict regolith breccia NWA 7034 and its 16 paired meteorites totaling a mess of ~941 g, including NWA 7533, are perhaps the most significant discovery among the martian meteorites in the past six years. These rocks show similar reflectance spectra and a bulk composition relative to the average crust (e.g., Agee et al., 2013; Cannon et al., 2015). The NWA 7034 meteorite group contains a variety of igneous clasts that include basalt, mugearite, trachyandesite, norite, gabbro, and monzonite (area sizes between 0.04 – 3 mm^2), some of which originate from different parent melts (Wittmann et al, 2015; Hewins et al., 2017; Santos et al., 2015). They also contain impact melt clasts (Wittmann et al., 2015), at least one of which has the same composition as the surface Gusev basalt Humphrey (Udry et al., 2014). The clasts in Northwest Africa 7034 represent the early Noachian lithified portion of the regolith, which has undergone some hydrothermal activity (McCubbin et al., 2016; Nyquist et al., 2016). The variability in rock type and compositions of the different clasts observed in this breccia, including some sedimentary clasts (e.g., Wittmann et al., 2015), show that there are many lithologies in this meteorite not previously represented in the other martian meteorites. This polymict regolith breccia likely assembled by pyroclastic eruption(s) and/or impact event(s), then underwent lithification represented by a thermal event at ~1.5 – 1.2 Ga (Bridges et al., 2017; Goderis et al., 2016; McCubbin et al., 2016). Alternatively, Cassata et al. (2018) proposed that contact metamorphism occurred between ~1500 and 1200 Ma based on $^{40}Ar/^{39}Ar$ ages, possibly due to plume-related magmatism, with brecciation and lithification happening at ≤225 Ma.

Northwest Africa 7034 igneous clasts contain the oldest dated martian minerals, which are zircons >4.3 Ga up to 4,476 ± 1 Ma, with a minimum source model age of 4,547 Ma, suggesting the formation of an extremely old enriched primordial crust, as the last stage of magma ocean crystallization (Bellucci et al., 2018; Bouvier et al., 2018; McCubbin et al., 2016; Nyquist et al., 2016). The fact that some alkaline clasts have crystallization ages of ~4.4 Ga show that alkaline magmatism occurred early in martian history, possibly due to early partial melting of mantle or contamination of primary magmas by the early alkali-rich martian crust (McCubbin et al., 2016). The regolith breccia was launched from Mars ~5 Ma ago and underwent relatively little shock metamorphism (between 5 – 15 GPa) (Wittmann et al., 2015). The shock history of the oldest zircons show that they underwent a low-shock history, signifying that the giant impact period on Mars, including the Borealis impact, formed before 4.48 Ga, and represents a maximum age for habitable conditions (Cassata et al., 2018; Moser et al., 2019).

2.3. Secondary processes recorded by meteorites

Meteorites are invaluable in our understanding of the geology of Mars. However, they have undergone secondary effects that have modified the chemistry that is either related to Mars, such as alteration (e.g., Beard et al., 2013; Bridges et al., 2001; Bridges & Schwenzer, 2012; Leshin & Vicenzi, 2006), mass independent fractionation of S in the surface environment (Franz et al., 2014), and shock (e.g., Fritz et al., 2005), or that are unrelated to

martian processes: i.e., terrestrial alteration (e.g., Crozaz et al., 2003). While these secondary processes may pose challenges for interpreting primary processes, nevertheless they are useful for understanding surface processes acting on Mars. Terrestrial alteration processes will not be recorded in returned samples, reducing complication from these effects. However, some of them might display evidence for shock metamorphism from previous impacts at the martian surface.

2.3.1. Terrestrial alteration

Most martian meteorites were found in hot (NWA) and cold (Antarctica) deserts, which allow terrestrial alteration and weathering to occur in these rocks. Although martian meteorites found in Antarctica have terrestrial ages two orders of magnitude older than NWA meteorites (mean age of 30 ka), the latter are more weathered than the cold desert rocks, due to ice limiting interaction with liquid water (Sharp et al., 2019). Chemical alterations are more problematic for analyses, for example evaporites (Mg- and Ca-carbonates, sulfates such as barite) are typically observed in fractures (Bland, 2001; Wadhwa et al., 2020). Through terrestrial alteration, bulk composition can be enriched in Ba, Sr, U, and Ce, and possibly the light rare earth elements (Crozaz et al., 2003).

2.3.2. Shock metamorphism

Shock features can change primary physical and chemical characteristics of the rocks. During ejection from Mars, ejected samples undergo shock metamorphism, which involves mineral deformation (twinning, mosaics, planar fractures) and amorphization of plagioclase (forming a diaplectic glass known as maskelynite), formation of shock melt, olivine reduction to Fe-nano particles, modification of the primary volatile content of apatite, and formation of high pressure minerals, such as ringwoodite [Mg_2SiO_4], tissintite [$(Ca,Na,)AlSi_2O_6$], tuite [γ-$Ca_3(PO_4)_2$], and coesite [SiO_2](Fritz et al., 2005; Sharp et al., 2019; Walton et al., 2014; Walton et al., 2012). Shock metamorphism is highly variable in martian meteorites, both between samples and within them. The lowest shock pressures experienced by martian meteorites show that at least 5 to 14 GPa is required to eject martian material from the surface (Fritz et al., 2005). There are several specimens with crystalline plagioclase, including NWA 4480, NWA 10416 (Walton et al., 2016), NWA 8159 (Sharp et al., 2019), and NWA 12241 (Udry et al., 2020) suggesting that these specimens were subjected to lower shock pressures than other meteorites where all of the plagioclase has been converted to diaplectic glass. Thus, most shergottites show higher shock pressures >19 GPa (Fritz et al. 2005), and rarely up to 70 – 90 GPa (Kizovski et al., 2019). Nakhlites have undergone limited shock, and contain crystalline plagioclase, although they can contain twinned augite (Treiman, 2005). In a given meteorite, the greatest effect of shock is often localized in glassy to partially-crystalline melt veins or pockets (e.g., Walton et al., 2014). Melt pockets are now understood to represent the former locations of void spaces or fractures (e.g., Sharp et al., 2019; Walton et al., 2014), providing an explanation for the implantation of atmospheric gases into these meteorites, most likely during the event that ejected them from Mars (Walton et al., 2007). The localization of shock effects and the short duration of shock largely negates arguments that shock features erase original chemical zonation and/or isotopic equilibrium (e.g., El Goresy et al., 2013) as demonstrated by Jones (1986), although care needs to be taken to avoid shock features (especially veins and pockets) for determining petrological and compositional characteristics of the meteorites.

2.4. Mars bulk silicate composition

Meteorites are a key constraint for the bulk composition of Mars. The Wänke and Dreibus models (Dreibus & Wanke, 1985; Wanke et al., 1994; Wanke & Dreibus, 1988) as well as the updated Taylor model (Taylor, 2013) have been the most widely used. By assuming refractory element abundances in the bulk silicate Mars (BSM) are the same as CI carbonaceous chondrites, these models use elemental compositions of martian meteorites to reconstruct the composition of BSM. Taylor (2013) suggested, as confirmed by earlier studies, that Mars is rich in FeO compared to the other inner planets, suggesting an FeO increase with heliocentric distance (FeO of Bulk Silicate Earth = 8.0 wt.%, McDonough & Sun, 1995). The Mars bulk H_2O is slightly depleted compared to Earth, with 300 ± 150 versus 500 ppm on Earth, and similar D/H. The martian volatile budget indicates that Mars likely accreted from inner solar system material (Taylor, 2013). Recently, Yoshizaki & McDonough (2020) suggested that CI chondrites do not represent the composition of Mars, and only use shergottite compositions and spacecraft data to determine the BSM. These authors show that Mars is systematically depleted in moderately volatile elements and enriched in refractory lithophile elements at 2.26 times higher than in CI chondrites. According to this study, the martian core contains light elements with ≤7 wt.% of S, less than previously suggested, but contains O (5.2 wt.%) and H (0.9 wt.%) (Yoshizaki & McDonough, 2020). The martian mantle is more oxidized and has a lower Mg# [= molar MgO/(MgO + FeO)] than the Earth mantle with a Mg# of ~0.79 (versus 0.88 on Earth; McDonough & Sun, 1995) for a FeO content of 14.7 ± 1.0 w.t% (versus 18 wt.% in Taylor, 2013 model) in the BSM.

2.5. Low-temperature alteration martian surface processes

Orbiters, landers, and rovers have shown geomorphological and mineralogical evidence of the presence of former liquid water on Mars as well as present ice in the polar caps and within the subsurface. Some hydrous minerals present in martian meteorites, like amphibole and apatite, are primary minerals and formed from crystallization of magma. However, most hydrous minerals in martian meteorites were formed through interaction with water occurring on the martian surface or subsurface. The compositions, textures, and ages of aqueous alteration can provide insights into the hydrologic history of Mars.

To distinguish martian from terrestrial alteration features and textures in meteorites, alteration minerals should ideally be older than the ejection events (e.g., cross cut by shock melt veins), and/or have documented martian compositions (Leshin & Vicenzi, 2006). Variable bulk rock and mineral δD values represent some combination of mantle reservoir(s) and/or near-surface/atmospheric reservoirs with δD values approaching those analyzed at the martian surface (> 5000 ‰; Villanueva et al., 2015; Webster et al., 2013) supporting a martian provenance (Hallis & Taylor, 2011; Liu et al., 2018; Usui et al., 2012).

All types of martian meteorites show variable degrees of martian alteration. Allan Hills 84001 includes ~1% of carbonate rosettes that have a wide range of compositions dated at 3.9 Ga (Borg & Drake, 2005). These carbonates likely formed from precipitation of an aqueous fluid or evaporative brine implying that water/rock interaction occurred during the Noachian (Beard et al., 2013; McSween, 2019; Velbel, 2012). Northwest Africa 7034 and pairs contain accessory pyrite that might have formed through hydrothermal activity under reducing conditions, possibly triggered by the 1.4 – 1.5 Ga thermal event (Liu et al., 2016; McCubbin et al., 2016; Wittmann et al., 2015). However, based on zircon compositions, Guitreau & Flahaut (2019) proposed an average alteration age of 227 Ma, close to the impact age suggested by Cassata et al. (2018). Some clast protoliths in NWA 7034 have undergone fluid-rock interactions at higher temperatures (>100ºC), before the brecciation impact event (Liu et al., 2016).

Nakhlites have undergone variable degrees of aqueous alteration evidenced by a wide variety of alteration minerals: the presence of iddingsite in fractures, Fe-rich carbonates (siderite), phyllosilicates, halite, gypsum, anhydrite, and pyrite/marcasite (Bridges & Grady, 1999; Day et al., 2006; Gillet et al., 2002; Hallis et al., 2014; Jambon et al., 2010; Lee et al., 2018; Tomkinson et al., 2015; Treiman, 2005; Velbel, 2012; Velbel, 2016). Iddingsite is ubiquitous in nakhlites and a product of hydrous alteration of olivine. It consists of a mixture of smectite, Fe-oxyhydroxides, silica, and salts. Localized alteration of sulfides is observed as hematite when in contact with mesostasis, except when sulfides are armored by Fe-rich pyroxenes (Day et al., 2006). The alteration of the different nakhlite samples is thought to be ~633 Ma based on iddingsite dating, possibly lasting from as little as 1 to 10 months (Borg & Drake, 2005; Changela & Bridges, 2010). Daly et al. (2019) recently proposed that aqueous alteration was aided through fracturing and brecciation by shock.

Finally, shergottites and chassignites are the meteorites that show the least alteration, and include Ca-, Mg-, and Fe-Mn-carbonates, chlorite, illite, and smectite (Leshin & Vicenzi, 2006; Stoker et al., 1993), dated between 1 and ~600 Ma (Borg & Drake, 2005; Chen et al., 2015). Recent studies of the olivine-phyric shergottite Tissint, which take advantage of the fact that it was recovered soon after its 2011 fall, and thus precluding terrestrial effects, demonstrate that shock melt pockets contain a cryptic signature of near-surface martian alteration, as evidenced by higher H_2O and Cl concentrations and δD and $\delta^{37}Cl$ isotopic compositions (Chen et al., 2015; Kuchka et al., 2017; Williams et al., 2016). Similar trends have also been observed in the shergottites Elephant Moraine (EETA) 79001 and Larkman Nunatak (LAR) 06319 (Liu et al., 2018; Usui et al., 2015). Collectively, these studies suggest small amounts of low-temperature alteration by water in contact with surface or atmospheric reservoirs, within fractures or voids that collapsed upon impact to form shock melt pockets (Kuchka et al., 2017; Liu et al., 2018).

It is apparent that shergottites and nakhlites did not undergo extensive leaching or low-temperature major element compositional changes, implying low water-rock interaction in these samples (Chen et al., 2015; Daly et al., 2019; Treiman et al., 1993). Similar to other meteorites, ALH 84001 also underwent relatively short lived and low water-rock ratio interaction, based on carbonate composition (Melwani Daswani et al., 2016). Although not pervasive, aqueous alteration has affected the martian meteorites from at least the early Noachian to the late Amazonian. The presence of liquid water throughout most of martian geologic history is consistent with surface data (Carr & Head, 2010), although the results from olivine-phyric shergottites provide insights into subsurface water chemistry over the past 600 Ma (Liu et al., 2018).

3. Igneous emplacement of martian magmas

The diversity in textures and mineralogies observed in martian meteorites indicate various emplacement processes close to the surface of Mars. Although textures and mineralogies can be inferred from observations of surface basalts, the analyses of textures and mineral compositions is much more accurate when conducted on samples in laboratories on Earth. The current number of martian meteorites and increasing number of ejection age determinations have allowed groupings of meteorites into different ejection sites and volcanic systems, and thus, provide more constraints on the evolution of their magmas and volcanic systems. Two examples of proposed co-genetic relationships include the nakhlite-chassignite association, where complementary igneous compositions and crystallization and ejection ages all imply that they originate from the same or a similar volcano-magmatic edifice on Mars (e.g., McCubbin et al., 2013; Udry & Day, 2018). Another is represented by a group of shergottite specimens that have identical ejection ages at 1.1 Ma and similar geochemical and

552 isotopic characteristics, perhaps representing a magmatic center active for at least 2 Ga (e.g.,
553 Lapen et al, 2017).
554
555 **3.1. Evolution and emplacement of shergottites**
556
557 Based on bulk major element compositions, shergottites from enriched, intermediate,
558 and depleted sources have been calculated to originate from mantle sources with anomalous
559 mantle potential temperatures (~1750˚C) compared to Noachian rocks from Gale crater
560 (~1450˚C), and thus represent products from a hot mantle plume (Filiberto, 2017). The large
561 number of shergottite specimens enable a better understanding of how the different sub-types
562 (poikilitic, gabbroic, basaltic, and olivine-phyric) were emplaced in the martian crust and
563 surface; a schematic representation is presented in Figure 6.
564 Olivine-phyric shergottites contain zoned olivine megacrysts (usually above > 0.5 mm
565 in length) that co-crystallized at depth within magma staging chambers, likely close to the
566 base of the crust, with low-Ca pyroxene phenocrysts and chromite (although co-crystallization
567 might not occur in the case of xenocrystic olivine). These crystals were entrained in an
568 ascending magma, which then erupted at the surface or was emplaced in the near-surface
569 hypabyssal environment. At this point, Fe-rich rims formed on olivine megacrysts and high-
570 Ca rims on pyroxene phenocrysts, followed by crystallization of plagioclase along with late-
571 stage accessory phases (e.g., Fe-Ti oxides, phosphates, sulfides) as the groundmass. The
572 olivine megacrysts in olivine-phyric shergottites can be phenocrystic, xenocrystic, or
573 antecrystic depending on the association with the groundmass in the rock. Some of the
574 olivine-phyric shergottites represent the closest approximation of primary mantle derived
575 magmas (e.g., Yamato-980459, NWA 5789, NWA 6234; Musselwhite et al., 2006; Gross et
576 al., 2011; Gross et al., 2013), although most have undergone some degree of crystal sorting in
577 magma staging chambers at depth or during ascent to the surface resulting in either loss or
578 addition of olivine macrocrysts (e.g., NWA 1068; Filiberto et al., 2010).
579 Poikilitic shergottites are characterized by coarse-grained (>1 cm in some cases) large
580 low-Ca pyroxene crystals with high-Ca rims enclosing olivine and chromite chadacrysts. As
581 with olivine-phyric shergottites, these phases likely crystallized close to the crust-mantle
582 boundary. Pyroxene oikocrysts were entrained and transported to shallower depths during
583 magma ascent, at which point additional pyroxene and olivine co-crystallized (Combs et al.,
584 2019; Howarth et al., 2014; Howarth et al., 2015; Rahib et al., 2019). The high abundance of
585 olivine with resultant high bulk-rock MgO contents of the poikilitic shergottites clearly
586 indicate significant accumulation of olivine during their emplacement in the crust and these
587 meteorites do not represent primary mantle melts. Plagioclase, along with accessory phases,
588 then crystallized during emplacement as shallow sills.
589 Basaltic and gabbroic shergottites form from relatively evolved magmas that have
590 undergone previous stages of olivine crystallization and fractionation and complete loss of
591 olivine phenocrysts from the system. They are marked by pyroxene crystallized at depths,
592 possibly within the same magma staging chambers where olivine fractionation occurred,
593 followed by subsequent plagioclase and accessory mineral crystallization during emplacement
594 at the surface as a flow or within the near-surface hypabyssal environment. Although most
595 shergottites show some degree of accumulation of early-formed phases (olivine and
596 pyroxene), most basaltic shergottites likely erupted onto the surface as lava flows (Liu et al.,
597 2016). As a result of pyroxene accumulation, most basaltic shergottites do not represent a
598 liquid composition, with some rare exceptions (e.g., Queen Alexandra Range — QUE —
599 94201; Kring et al., 2003; McSween et al., 1996).
600 Petrogenetic relationships between shergottite sub-types have been constrained on the
601 basis of mineralogy, bulk chemistry and inferred parental melt composition, and isotopic

characteristics. According to their mineral, bulk, and isotopic compositions, the different sub-types of shergottites are likely petrogenetically linked (Rahib et al., 2019; Treiman & Filiberto, 2014). Based on texture, isotopic composition, and mineralogy, poikilitic shergottites are linked through fractionation to basaltic and olivine-phyric shergottites and might originate from the same magmatic systems (Filiberto et al., 2018; Rahib et al., 2019; Udry et al., 2017). Specifically, poikilitic shergottites may have formed from fractionation of an originally olivine-phyric shergottite-like magma through fractionation of olivine within staging chambers at depth; early pulses of magma ascending from staging chambers incorporated predominantly olivine and formed olivine-phyric shergottites at the surface, whereas later ascending magmas incorporated more pyroxene oikocrysts and formed the poikilitic shergottites at the surface (Coombs et al., 2019). Basaltic shergottites may also have formed from an olivine-phyric shergottite magma, through fractionation of olivine or lack of olivine entrainment (Combs et al., 2019; Filiberto et al., 2012; Treiman & Filiberto, 2014; Udry et al., 2017). This process may explain the low-Al basalts, with high-Al basalts formed through further fractionation of pyroxene. Gabbroic shergottites are also likely linked to basaltic shergottites. For example, the gabbroic NWA 7320 originated from a common volcanic system with the basaltic shergottites, Los Angeles and NWA 856, based on similar mineralogy and isotopic composition (Udry et al., 2017). Northwest Africa 7320 represents a sub-volcanic cumulate version of a basaltic shergottite that erupted at the surface. Some of the gabbroic meteorites could represent the feeder dike system that fed the lava flows represented by the basaltic shergottites. The petrogenetic link between groups of shergottites is also supported by the fact that ~20 depleted shergottites, including basaltic and olivine-phyric shergottites, and the augite-rich types (NWA 7635 and 8159), have ejection ages within error of 1.1 Ma, suggesting that they originated from the same long-lived volcanic system, active from at least 327 to 2403 Ma (Brennecka et al., 2014; Lapen et al., 2017).

Due to lack of calibrations for martian conditions, few geobarometers can be used to constrain the depth of crystallization of martian meteorite phenocryst/megacryst phases. Pyroxene Ti/Al can help constrain a range of pressures of crystallization (not an exact pressure, as it is not fully calibrated for Mars; Filiberto et al., 2010; Nekvasil et al., 2007). The application of this geobarometer to various shergottites and chassignites suggest that formation of staging chambers at the crust/mantle boundary may be widespread on Mars, possibly leading to the formation of the various shergottite lithologies (Combs et al., 2019; Dunham et al., 2019; Filiberto, 2017; Howarth et al., 2018; Nekvasil et al., 2004; Rahib et al., 2019; Udry et al., 2017). Minor element compositions in pyroxene in nakhlites also suggest that they could have formed at the bottom of the martian crust (McCubbin et al., 2013; Udry & Day, 2018). As such, there may be a large quantity of pyroxenite (and possibly dunite or wehrlite) cumulates that underplate the martian crust and in the martian lithosphere, which represent materials from these staging chambers.

3.2. Evolution and emplacement of nakhlites/chassignites

In contrast to shergottites, which originated from different localities, the nakhlite and chassignite meteorites have been inferred to be derived from a large igneous pile. A recent comprehensive study by Udry and Day (2018) shows that nakhlites and chassignites were likely emplaced as various lava flows and/or hypabyssal sills according to their different mineralogies, cooling rates, and qualitative and quantitative textures, similar in many ways to volcanic emplacement on Earth (Balta et al., 2017; Corrigan et al., 2015; Daly et al., 2019; Jambon et al., 2016; Udry & Day, 2018). At least four eruptive events for the nakhlites are suggested by their $^{40}Ar/^{39}Ar$ ages, that vary between 1415 ± 7 Ma (Yamato 000749) to 1322 ± 9 Ma (Lafayette) (Cohen et al., 2017).

3.3. Link between shergottites and nakhlites/chassignites?

Radiogenic isotope data of nakhlites as a whole are similar to depleted/intermediate shergottites. However, there are distinct differences that appear to preclude or complicate genetic relationships between shergottites (including ALH 84001) and nakhlites. For example, all shergottites plot as a linear array on a $^{142}Nd/^{144}Nd_{(measured)}$ versus $^{143}Nd/^{144}Nd_{(present\ day)}$ diagram (e.g., Debaille et al., 2007; Caro et al., 2008; Borg et al., 2016; Lapen et al., 2017; Figure 7). Regardless of whether the linear array represents a mixing line between depleted and enriched mantle sources (e.g., Debaille et al., 2007; Lapen et al., 2017) or that the slope of the array has age significance (e.g., Borg et al., 2016), the nakhlites do not plot on this array requiring the nakhlite mantle sources to have a different early evolution than shergottite sources. Based on ^{176}Lu-^{176}Hf, ^{146}Sm-^{142}Nd, ^{147}Sm-^{143}Nd, and W isotope compositions of nakhlites, Debaille et al. (2009) proposed a model of early majoritic garnet fractionation that explains the apparent decoupling of W, Hf, and Nd isotopes observed in these meteorites and not shergottites. Given that there is as yet no evidence for isotopic mixing between shergottite and nakhlite mantle sources, these reservoirs and partial melts from them seem to have remained isolated from one another during their petrogeneses.

However, based on their bulk trace element compositions, nakhlite, chassignite, and shergottite-like magmas are predicted to be produced from large plume-fed systems, despite the fact that these groups of meteorites show different mineralogies and source compositions (Day et al., 2018). It has been proposed that shergottites and nakhlites represent main shield and later metasomatized rejuvenated magmas, respectively, in a stagnant-lid regime (Day et al., 2018). This process is represented in figure 8. Due to eruption of a large volume of shergottite lavas during the main shield period, load is emplaced unevenly on the underlying lithosphere, leading to flexure and the development of a flexural bulge outboard of the volcanic edifice. Flexural moats and bulges are observed on Earth in the Hawaiian-Emperor chain volcanoes and also occur, based on gravity, in the Tharsis volcanic province on Mars (e.g., Genova et al., 2016; Sandwell et al., 2014). As with terrestrial rejuvenated lavas, a previously depleted mantle, which is required for the source of nakhlites based on their Sr-Nd isotope systematics, has to be metasomatized in order to induce localized partial melting through decompression during lithospheric flexure. Nakhlite- and chassignite-like melts would correspond to rejuvenated magmas (Day et al., 2018).

4. The interior of Mars is poorly mixed

Martian meteorites allow the timing of planet-formation processes to be elucidated using isotopic and elemental compositions inherited from their source reservoirs. Both Earth and Mars have geochemically and isotopically distinct components, but Mars does not have plate tectonics that would have facilitated mixing and dilution of primordial components. Thus, Mars retains a higher resolution record of mantle heterogeneities produced during early planetary differentiation. Mantle heterogeneities are assessed using trace elements and isotopic compositions, including $^{146,147}Sm$-$^{142,143}Nd$, ^{182}Hf-^{182}W, $^{176}Lu/^{177}Hf$, U-Pb, ^{87}Rb-^{87}Sr, and ^{187}Re-^{187}Os, as well as redox conditions (Bellucci et al., 2018; Brandon et al., 2012; Day et al., 2018; Debaille et al., 2008, 2009; Herd, 2003; Herd et al., 2017; Lapen et al., 2017; Tait & Day, 2018; Wadhwa, 2001). At least six different reservoirs have been proposed on Mars, including a mixture of three for shergottites and ALH 84001 (e.g., Lapen et al., 2010; 2017; Figure 4), one for the nakhlites and chassignites (e.g., Debaille et al., 2009), one for NWA 8159 (e.g., Bellucci et al., 2020) and at least one for some components in NWA 7034 (Armytage et al., 2018). In this section, we describe these different sources, their timing of

formation, and the early global processes for Mars, including accretion and differentiation, which can only be determined using samples.

4.1. Shergottite reservoirs

Shergottites represent the mixture of at least three endmember mantle components that can describe the compositional array of all shergottites and ALH 84001 (Fig. 4; Debaille et al., 2008; Lapen et al., 2017). When plotted on bivariate diagrams, the calculated mantle source compositions of shergottites and ALH 84001 strongly define mixing hyperbolas or mixing lines, depending on the data. Bivariate plots of $^{147}Sm/^{144}Nd$ and $^{87}Rb/^{86}Sr$ source ratios are predicted to be produced from large plume-fed systems, of depleted, intermediate, and enriched shergottites (and ALH 84001) define an apparent two-component mixing hyperbola and two-component mixing line, respectively (e.g., Borg et al., 2003; Lapen et al, 2017). Bivariate plots of $^{176}Lu/^{177}Hf$ and $^{147}Sm/^{144}Nd$ source ratios, however, indicate mixtures of at least three components. Using mantle cumulate and residual liquid compositions calculated from the progressive Mars magma ocean crystallization model of Debaille et al. (2008), the most depleted component (highest $^{176}Lu/^{177}Hf$ and $^{147}Sm/^{144}Nd$ source ratios; 0.08 and 0.4, respectively) might represent mantle cumulates that constitute the depleted Mars upper mantle mantle. Another depleted component might represent shallower and more evolved mantle cumulates with less elevated $^{147}Sm/^{144}Nd$ and $^{176}Lu/^{177}Hf$ source ratios than earlier-formed deeper cumulates. The enriched endmember can be modeled as dominated by a trapped residual liquid component in the upper mantle (e.g., Lapen et al., 2010) with $^{176}Lu/^{177}Hf$ and $^{147}Sm/^{144}Nd$ source ratios of approximately 0.017 and 0.17, respectively (Lapen et al., 2017; Figure 4). These data imply a hybridized martian mantle. In addition to the shergottite source systematics shown by the Lu-Hf, Sm-Nd, and Rb-Sr data, the Re-Os and U-Pb isotope systems also follow the predicted mantle source mixing where depleted and enriched endmembers can be mixed to produce the compositional variations observed in shergottites (Bellucci et al., 2018; Brandon et al., 2012; Day et al., 2018; Debaille et al., 2008, 2009; Herd, 2003; Herd et al., 2017; Lapen et al., 2017; Tait & Day, 2018; Wadhwa, 2001). These mantle source endmembers also have differences in redox conditions (oxygen fugacity, fO_2), resulting in correlations between calculated primary fO_2 in the shergottites, ITE abundances, and radiogenic isotope compositions (Figs. 9, 10) (e.g., Borg et al. 2002, 2003, 2016; Brandon et al. 2012; Brennecka et al. 2014; Combs et al. 2019; Debaille et al. 2008; Ferdous et al. 2017; Herd 2003; Lapen et al. 2017; McSween 2015; Nyquist et al. 2001; Rahib et al. 2019; Shafer et al. 2010; Symes et al. 2008; Tait and Day 2018; Usui et al. 2010; Wadhwa 2001). Finally, the shergottite components have heterogeneous volatile contents, with 36 to 73 ppm H_2O in the enriched source and 14 to 23 ppm H_2O in the depleted source (McCubbin et al., 2016), discussed below in section 4.5.

Although it is accepted that the depleted components are located in the mantle, the origin of the enriched component is still debated, and could be located in the crust or mantle (Borg & Draper, 2003). Recent consensus leans toward an enriched mantle source — or sources. If the enriched source were the crust, it would signify that crustal assimilation has occurred. However, assimilation is not consistent with major element, isotopic compositions, and redox conditions of shergottites (Armytage et al., 2018; Brandon et al., 2012; Ferdous et al., 2017; Herd, 2003; Symes et al., 2008; Tait & Day, 2018). Peters et al. (2015) proposed that the trace element compositions indicate that crustal recycling back into the mantle, possibly through delamination — due to the higher density of the lower crust (Papike et al., 2013), might be responsible for the enriched shergottite source. Regardless of their origin, shergottites represent variable mixtures of these endmember compositions. For example, Combs et al. (2019) showed that the enriched shergottites Los Angeles, NWA 7320, NWA

856, and NWA 10169 likely originated from a different mantle source endmember mixture than the other enriched shergottites based on their Lu/Hf isotopic compositions. In addition, the depleted reservoir might also be locally heterogeneous based on U/Pb and Sm/Nd ratios (Moriwaki et al., 2020).

The early Amazonian shergottite NWA 8159 formed from a depleted mantle source (Herd et al., 2017) that is distinct from the depleted shergottites based on Cr, W, Nd, and Pb isotopic studies (Bellucci et al., 2020; Herd et al., 2017). While NWA 8159 shares some similarities with NWA 7635, including crystallization age, mineralogy, REE compositions, and ejection age – suggesting they may be launch-paired – further studies are required to discern whether they are derived from the same mantle source and are petrogenetically related (Herd et al., 2017).

Shergottite sources show diversity in isotopic and elemental compositions, but also in oxygen fugacity (fO_2), representing their redox history. Shergottites show a large variability in redox conditions, indicating redox heterogeneity of the interior. Based on fewer samples, it was noted that shergottite fO_2 correlates with their isotopic compositions and bulk REE enrichment (Herd, 2003; Herd et al., 2002; Wadhwa, 2001). The discovery and study of diverse new shergottites complicates the simplicity of the original correlations. However, fO_2 does correlate with source compositions once the effects of ascent and eruption are taken into account (e.g., Castle & Herd, 2017). Oxygen fugacity, and thus, redox history, is determined using major and/or trace element-based oxybarometers applied to the compositions of different mineral assemblages (see Herd, 2008 for a review). It is important to calculate the fO_2 of early-crystallizing and late-crystallizing mineral assemblages, as these mineral assemblages will represent different stages of crystallization, and thus, different set of conditions. Olivine-phyric and poikilitic shergottites show at least two different stages of crystallization. By measuring the early- and late-stage mineral assemblages, it was shown that an increase in fO_2 (up to ~3 log units relative to the quartz-fayalite-magnetite – QFM – solid oxygen buffer) occurred from early- to late-stage crystallization in all measured olivine-phyric shergottites. This increase in fO_2 implies that most shergottites underwent degassing and/or auto-oxidation during magma ascent (Castle & Herd, 2017, 2018; Howarth et al., 2018; Rahib et al., 2019). Evidence for the degassing process suggests that volatiles were present early in the shergottite parental magma, although the suite of volatiles responsible for the oxidation have yet to be elucidated (Balta et al., 2013; Castle & Herd, 2017; Combs et al., 2019; Howarth et al., 2014; Howarth et al., 2018; Howarth & Udry, 2017; Peslier et al., 2010; Rahib et al., 2019; Shearer et al., 2019). Figure 10 provides a schematic representation of the correlation between fO_2 and La/Yb ratio — a proxy for incompatible element enrichment. The fO_2 trends for early-crystallizing assemblages in poikilitic shergottites, olivine-phyric, and basaltic shergottites increase from depleted to enriched shergottites, demonstrating that the different shergottite reservoirs have different fO_2. These trends are parallel, especially poikilitic and basaltic trends, suggesting a link between the different shergottite groups. Note that subsolidus Fe-Mg exchange might have occurred in early-crystallizing olivine and chromite in poikilitic shergottites, complicating calculated fO_2 for these rocks (Walton et al., 2012).

4.2. Nakhlite/chassignite reservoir

An isotopically uniform mantle source reservoir is inferred for nakhlites and chassignites, which has been ITE depleted for most of Mars history (high $^{176}Lu/^{177}Hf$ and $^{147}Sm/^{144}Nd$, and low $^{87}Rb/^{87}Sr$ and $^{187}Re/^{188}Os$). The $\varepsilon^{143}Nd_{(present\ day)}$ versus $\varepsilon^{142}Nd_{(measured)}$ of nakhlites (Debaille et al., 2009; Figure 7) indicate limited variability in compositions that are distinct from the shergottite source mixing line. This source reservoir is more depleted in

HREE than shergottites and could have experienced early garnet fractionation (Debaille et al., 2009; Treiman, 2005). According to $\delta^{34}S$ compositions and secondary phases indicative of alteration, some nakhlite samples record hydrothermal processes and assimilation of martian regolith, and possibly assimilation of an enriched mantle component based on their $^{187}Os/^{188}Os$ composition (Franz et al., 2014; Mari et al., 2019). The nakhlite source seems to have undergone variable degrees of metasomatism (= change in bulk composition due to introduction of fluids). Based on the calculated compositions of the nakhlite parental melt, the nakhlite and chassignite sources could have been enriched in K through metasomatism (Goodrich et al., 2013; Ostwald et al., 2020). This form of metasomatism has also been suggested for the source of surface Gale crater rocks (Stolper et al., 2013; Treiman et al., 2016; Udry et al., 2014), and thus might be a widespread process in the shallow martian interior.

4.3. Polymict regolith breccia source

The mantle sources of some igneous components in the regolith breccia NWA 7034 and its paired meteorites are different from the source of the other martian meteorites, primarily because it is a polymict breccia with clasts of a variety of material types. Nevertheless, their isotopic composition (low $^{147}Sm/^{144}Nd$ and $^{176}Lu/^{177}Hf$) is consistent with an ancient LREE-enriched crust, which is distinct from the enriched shergottite source (Armytage et al., 2018; Kruijer et al., 2017; Nyquist et al., 2016). In addition, the Pb isotopic compositions of the paired regolith breccias shows that a previously unknown enriched reservoir in $^{207}Pb/^{204}Pb$ is present in the martian interior, and is possibly crustal (Bellucci et al., 2016). Alkali basalt clasts in Northwest Africa 7034 are also highly oxidized compared to all other martian meteorites with fO_2 of QFM+3 (calculated from ilmenite-magnetite pairs, Santos et al., 2015). As noted above, clasts within NWA 7034 (and paired rocks) provide unprecedented insights into the nature of the early martian crust, and shows that it was isotopically and chemically distinct from the sources of the other martian meteorites.

4.4. Early martian history and magma oceanography

Mars accretion and core formation occurred before the accretion of the Earth, estimated between 7 – 10 Ma (Fig. 5, Dauphas & Pourmand, 2011; Foley et al., 2005; Kleine et al., 2004; Kruijer et al., 2017) after solar system condensation of calcium-aluminum-rich inclusions (CAIs) at ~4567 Ma (Amelin, 2002; Connelly et al., 2017; Connelly et al., 2012). After an initial major phase of accretion, terrestrial planets are widely considered to have undergone global and deep melting, resulting in a magma ocean, referred here for Mars as the MMO (martian magma ocean) (Elkins-Tanton et al., 2003). The latest estimates of the duration of crystallization of the MMO are from 10 to 25 Ma after solar system condensation (Kruijer et al., 2017), but could have lasted up to 100 Ma (Debaille et al., 2009; Elkins-Tanton, 2005). Following crystallization of the MMO and the formation of solid cumulates, mantle overturn occurs. Mantle overturn is induced from the final crystallizing layers, which are inferred to be rich in Fe and incompatible elements forming near the top of the MMO, and are denser compared to earlier-crystallizing layers — they will therefore sink into the mantle (Elkins-Tanton et al., 2003). The solid cumulates that are formed during initial crystallization are then moved within the mantle during overturn. During overturn, crystallized MMO areas can melt adiabatically.

Large-scale mantle reservoirs, including the different sources of martian meteorites, likely formed during silicate differentiation associated with MMO solidification and overturn (Bouvier et al., 2018; Debaille et al., 2008; 2009; Kruijer et al., 2017). Combined W and Nd

isotopic compositions of shergottites, ALH 84001, and NWA 7034, suggest a single differentiation event between 25 and 40 Ma after solar system condensation that established the mantle sources for the meteorites (Kruijer et al. 2017). Formation of components recorded in these rocks need not have been contemporaneous, nor do all enriched shergottite components need to be identical on this basis (Kruijer et al. 2017). The cumulate components of the MMO represent the depleted component(s), whereas the enriched component(s) are likely the last dregs of MMO crystallization (e.g., Borg & Draper, 2003; Lapen et al., 2010; Moriwaki et al., 2020). Mixing of the two could have formed the intermediate reservoir (Borg et al. 2003). The depleted shergottite reservoir might also be locally heterogeneous based on U/Pb and Sm/Nd ratios (Foley et al., 2005) and coupled Lu/Hf and Sm/Nd source systematics (Lapen et al., 2017), possibly due to later events than the MMO, including further mixing of enriched and depleted source or local remelting (e.g., Tait & Day, 2018), or as produced directly from the MMO crystallization processes (Debaille et al., 2008). Differentiation histories were likely different between shergottites and nakhlites/chassignites based on the ^{182}Hf-^{182}W and ^{146}Sm-^{142}Nd systems (Bellucci et al., 2018), due to possible mantle overturn (Dauphas & Pourmand, 2011; Foley et al., 2005; Debaille et al., 2009) and late addition of material to the martian mantle. While nakhlites potentially record the mantle overturn (Debaille et al. 2009), this process is not obviously consistent with a metasomatized source for nakhlites proposed by Day et al. (2018), as the nakhlite depleted source was likely metasomatized by fluids later on, possibly due to plume impingement. The nakhlite mantle source likely formed before the shergottite source and might have formed during the first 10 – 25 Ma after CAI condensation (Borg & Drake, 2005; Debaille et al., 2009; Foley et al., 2005) and have different ^{182}W than shergottites. The source of ALH 84001 also formed early at ~20 Ma (Kruijer et al., 2017), which is related to, and perhaps identical with, the enriched shergottite source endmember (Lapen et al., 2010).

Solid-state MMO overturn and associated decompression melting could have formed the martian crust between 20 and 100 Ma after solar system condensation (Bouvier et al., 2018; Debaille et al., 2008; Kruijer et al., 2017). The more recent estimate of crustal formation (~4547 Ma) was calculated using the oldest zircons found in NWA 7034. This age implies that an enriched andesitic-like crust formed extremely early in Mars history at the last stages of magma ocean crystallization (Bellucci et al., 2018; McCubbin et al., 2016; Nyquist et al., 2016). The source of NWA 7034 could have formed up to ~40 Ma after CAI condensation; note that as NWA 7034 is a polymict breccia, and might originate from several sources (Kruijer et al., 2017). Furthermore, the similarity in W-Nd isotopic composition between NWA 7034, ALH 84001, and enriched shergottites suggest that Mars is relatively simple in terms of W and Nd isotopic reservoirs. Little compositional mixing has occurred throughout the entire geologic history of Mars and thus the shergottite sources have not significantly changed since its formation due to the absence of vigorous convection, in particular, the lack of toroidal flow associated with transform boundaries (Kiefer, 2003).

4.5. Volatiles in the martian interior

The last ten years has seen a focus and significant debate about the pre-eruptive volatile content of martian igneous rocks. The problem came from the fact that bulk water contents of shergottites are lower than most terrestrial magmas (50 – 150 ppm) (Dreibus & Wanke, 1985; Leshin, 2000; Leshin et al., 1996), which originally lead to two schools of thought: martian magmas were drier than their terrestrial counter parts or martian magmas catastrophically degassed before eruption and were initially much wetter (Dann et al., 2001; Filiberto & Treiman, 2009; Herd et al., 2005; Lentz et al., 2001, 2001; McCubbin et al., 2012;

McSween et al., 2001; Nekvasil et al., 2007; Treiman, 1985; Treiman et al., 2006; Udry et al., 2016; Usui et al., 2012; Wilson & Head, 1981).

Constraining this discrepancy required new detailed analyses of apatite, amphibole, melt inclusions, nominally anhydrous minerals, and impact melts. Apatite is a ubiquitous but minor phase in most martian meteorites and the only primary volatile-bearing phase in shergottites. Apatite chemistry can reveal the primary volatile content of the parent magma, but only if: (1) significant crystal fraction did not occur; (2) the magma did not degas before apatite crystallization; (3) magma mixing did not occur; (4) the magma did not assimilate crustal material; (5) the magma did not interact with crustal fluids either during or after crystallization; or (6) the apatite was not affected by shock related processes (Howarth et al., 2015; McCubbin et al., 2016). Amphibole is a better recorder of magmatic volatiles than apatite (Hawthorne, 1983). However, amphibole is rare in martian meteorites and is only found in melt inclusions in a limited number of meteorites (McCubbin et al., 2013; Sautter et al., 2006; Treiman, 1985). Amphibole chemistry is complicated and requires complex modeling to calculate the parental magma and these models are not fully calibrated for martian magmas (Giesting et al., 2015; Giesting & Filiberto, 2014). Direct measurements of volatiles in magmas can be made on melt inclusions in olivine and pyroxene (Usui et al., 2012), but hydrogen can easily diffuse through the silicate host (Gaetani et al., 2012) and crystallization can cause element exchange between the melt inclusion magma and silicate host (Danyushevsky et al., 2000). Therefore, while melt inclusions can be used to constrain volatile contents of parent magmas, care needs to be taken before directly applying these measurements. Nominally anhydrous minerals, such as olivine and pyroxene, can contain tens to hundreds of ppm H_2O in the form of protons incorporated into their structural defects. The H_2O contents of olivine and pyroxene in martian meteorites has been shown to be similar to that of terrestrial olivine and pyroxene phenocrysts in basalts (see review of Peslier, 2010). In order to get accurate estimates of the primary H_2O contents of these nominally anhydrous minerals, the effects of degassing and shock metamorphism need to be carefully considered (e.g., Peslier et al., 2019). Finally, impact-melt hygrometers have also been developed to track the primary versus secondary sources of volatiles in martian meteorites, which indicate mixing between primary magmatic H_2O and crustal H_2O reservoirs (Chen et al., 2015; Liu et al., 2018).

Of the above-mentioned ways in which the volatile contents of martian magmas can be constrained, apatite has received the most attention. Using the constraints on apatite and amphibole petrogenesis discussed in the previous paragraph discarding any analyses that may have been affected by element mobility, Filiberto et al., (2016) and McCubbin et al., (2016) in companion papers attempted to constrain the pre-eruptive volatile (H_2O, Cl, and F) contents of the parent magma to shergottite meteorites and their source region. They specifically excluded the nakhlites from this calculation because the nakhlites have seen both high-temperature magmatic hydrothermal fluids and secondary low-temperature fluids that have altered the apatite chemistry (Bridges & Schwenzer, 2012; Filiberto, Treiman, et al., 2014; Giesting & Filiberto, 2016). These companion papers along with a follow up study (Filiberto et al. 2019), showed that shergottite magmas have 2.5 ± 1 times the amount of chlorine compared with terrestrial magmas and that they were not volatile saturated — e.g., they did not degas before eruption (at least those using these conservative filters). Instead shergottite magmas have water contents consistent with their bulk water contents (5 – 150 ppm water) and similar to terrestrial mid-ocean ridge basalts (Filiberto et al., 2016). Using these magmatic volatile contents, McCubbin et al. (2016) then calculated water contents of different source regions: a) 36 – 73 ppm H_2O for the enriched shergottite source and b) 14 – 23 ppm H_2O for the depleted shergottite source region. These values represent water contents for the shergottite source during the Amazonian. Based on nominally anhydrous minerals rather than

apatite, the mantle source sampled by the nakhlites has been estimated to have 59 – 184 ppm (Peslier et al., 2019). A recent study by Barnes et al. (2020) shows that the bulk martian crust (represented by NWA 7034 and ALH 84001) has likely had the same D/H composition for at least 3.9 Ga and that the D/H compositions of the enriched and depleted shergottite sources are heterogeneous. The crust likely represents a mixture of at least two mantle reservoirs. This study is further evidence that the enriched source of shergottites originate from the mantle. In contrast, Hu et al. (2020) suggests that shergottites represent the mixing of crustal (δD ~5000 – 6000‰) and magmatic water (δD = 0 ‰).

A major uncertainty for the volatile content of the martian interior remains what was the volatile content earlier in Mars' history (Filiberto et al., 2016). It is likely that earlier in Mars history, the interior was more volatile-rich in terms of water, halogens, carbon, and likely sulfur (e.g. Filiberto et al., 2016; McCubbin et al., 2016; Médard & Grove, 2008) and through time, volatile elements partitioned into the magma, as they are all largely incompatible elements during mantle melting, and then were lost to the crust and atmosphere during emplacement. Without plate tectonics and crustal recycling, there is no large-scale mechanism to replenish the interior with volatile elements, and thus the martian interior should have dried out through time. However, the extent to which this occurred, the exact volatile content of the Noachian mantle, and how heterogeneous the interior was remains largely unconstrained (see Filiberto et al. 2016b for a full review of open-ended questions).

5. What we still don't know

One of the main knowledge gaps for the martian meteorites is the locations on the surface from where they were derived. Comparison of martian meteorite ages with the crater chronology-based ages of surface units shows a distinct bias in the martian meteorite suite. This bias was recognized early in the study of martian meteorites, when the total number of recovered meteorites was low (e.g., Jones, 1989; Warren et al., 2004). A better understanding of the physics of ejection of the meteorites (e.g., Head, 2002), and considerations of shock effects and isotopic compositions (e.g., Walton et al., 2008) only strengthens this conclusion. It is apparent that the process of ejection of meteoroids from Mars is sufficiently violent as to favor young igneous lithologies.

Martian meteorites in the terrestrial collection were ejected from Mars between 0.7 Ma to 20 Ma, corresponding to ≥ 11 different events, as determined by isotopes such as ^{3}He, ^{10}Be, ^{15}N, ^{21}Ne, ^{38}Ar, ^{53}Mn, and ^{81}Kr (Herd et al., 2017; Herzog & Caffee, 2014; McSween, 2015; Nyquist et al., 2001; Wieler et al., 2016). Meteorites deriving from the same location on Mars will likely have the same ejection age, as it can be assumed, based on crater distribution on Mars, that a single impact event occurred to eject rocks from the same location. Some groups of martian meteorites likely originated from the same location. The nakhlites and chassignites have an ejection age of 11 Ma (Cohen et al., 2017), with the exception of NWA 5790, which has an ejection age of ~7.3 ± 0.4 Ma (Wieler et al., 2016). The latter ejection age suggests that two distinct ejection events could represent the same location on Mars. The depleted shergottites have an ejection of 1.1 ± 0.2 Ma (95% confidence), including at least 20 samples (Lapen et al., 2017). These are good examples of where ejection ages have allowed determination of groups of meteorites originated from similar locations and thus allow for more comprehensive studies of cogenetic magma systems. Long-lived volcanoes based on crater age counting (> 3 Ga, including Alba Mons, Biblis Tholus, Jovis Tholus, Uranius Mons, and Hecates Tholus) are well known on Mars; thus NWA 7635, NWA 8159, and the depleted shergottites may originate from one of them. Most of the rest of shergottites have ejection ages varying between ~2 and 5 Ma (Herzog & Caffee, 2014; Wieler et al., 2016)

To locate the possible source location of meteorites at the surface, crater features need to fit meteorite features, including the age of ejection and crystallization, the minerals present, and their modal abundances (e.g., Treiman 1995). For most meteorites, we expect young craters in Amazonian terrains. In addition, Bowling et al. (2020) recently showed that the size of crater can be linked to 'dwell times' (time spent by meteorites at high pressure during impact), determined by the high pressure mineralogy observed in meteorites. Less than 10% of the martian surface is younger than 1 Ga (Hartmann & Neukum, 2001), including Tharsis, Amazonis Planitia, and Elysium (Fig. 11). The higher elevation of these areas, and thus lower density of the atmosphere, lead to easier ejection of fragments to space. Oblique and rayed craters, which represent young and high ejection velocities craters with preserved impactites, are likely the best candidates (Artemieva & Ivanov, 2004; Fritz et al., 2005; Tornabene et al., 2006).

Several techniques have been attempted to try to determine meteorite source craters, including spectral matching (Hamilton et al., 2003; Ody et al., 2015), combined with crater counting (Mouginis-Mark et al., 1992; Werner et al., 2014), as well as impact modeling (Herd et al., 2017; 2018). Notably, spectral matching is hindered by dust coverage, especially for the Amazonian igneous terrains (e.g., Lang et al., 2009). Modeling using the iSALE shock physics code simulates dwell times and peak pressures of ejection of Mars-like basaltic target and constrains pre-impact burial depth (Bowling et al., 2020). A crater diameter range can be inferred from this model (Herd et al., 2018). Fewer than 20 >2.5 km diameter well-preserved potential source craters in igneous terrains of Amazonian ages were identified as possible sources for four representative meteorites (Zagami, Tissint, Chassigny, and NWA 8159; Herd et al., 2018); a subset of these are currently being mapped in detail to further assess their likelihood as source craters (Hamilton et al., 2020).

Various source craters have been proposed for martian meteorites, but none have been confirmed. Terrains proposed by Hamilton et al. (2003) match the mineralogy of some martian meteorites, but are not consistent with their ages nor associated with young source craters. Some craters were selected by Werner et al. (2014) and Ody et al. (2015), including Mojave crater; however, these authors assumed that shergottites are Noachian in age. Nakhlite source craters were proposed at Syrtis Major, Tharsis, and Zumba and Gratteri craters, located south of Tharsis (e.g., Mouginis-Mark et al., 1992; Hamilton et al., 2003; Harvey & Hamilton, 2005; Tornabene et al., 2006). Six <3 km rayed craters dated at 11 Ma were identified as possible sources of nakhlites (Kereszturi & Chatzitheodoridis, 2016). Daly et al. (2019) showed that nakhlites have undergone shock metamorphism before 633 Ma (time of aqueous alteration) and that the 11 Ma nakhlite source crater should have formed close to the impact occurring before 633 Ma. Nakhlites might also originate at a shield volcano flexural bulge (Day et al., 2018), but as of now, no craters in this geological context have been identified as the potential nakhlite source crater. Wittmann et al. (2015) proposes that the polymict regolith breccia NWA 7533 and paired (including NWA 7034) originate from the 6.9 km diameter, ~5 Ma old Gratteri crater.

6. What is the lithological variation on Mars?

Meteorites are currently the only samples that we have from Mars. They provide a context for silicate differentiation and mantle source formations, igneous fractionation and emplacement and evolution, and secondary processes, such as aqueous alteration. The bulk composition of Mars can only be determined using these samples. Early martian history is shown to have involved fast accretion and core formation compared to Earth. Discovery of new martian meteorites has revealed a diversity of sources and magmatic history, and that the martian interior is more heterogeneous than previously thought. Indeed, these finds point to

lithologies that we do not have that might reveal fundamental processes that we also do not know about in Mars. From the martian meteorites, we now know that Mars has a heterogeneous mantle, represented by various mantle sources, which have not significantly mixed since the differentiation of the martian magma ocean, due to the lack of plate tectonics and transform boundaries (Kiefer, 2003). The ancient crust is underrepresented in martian meteorites, but an old crustal reservoir is represented in the Noachian meteorite NWA 7034. Notably, this crust is not nearly as aqueously altered relative to what is inferred from orbital observations of Noachian terrains (Table S3; e.g., Bibring et al., 2005). The martian crust has contributed to volatile contents but not to trace element or isotopic compositions of meteorites. Meteorites have shown that Mars is mostly a basaltic planet, but other compositions, such as alkali-rich lithologies that formed very early in martian history, have been recently discovered via rover exploration (e.g., Filiberto, 2017). Various magmatic processes and compositions are reflected in martian meteorites, through their textures, mineralogy, and bulk compositions. Meteorites help us to understand processes during the Amazonian and show that lithologies such as shergottites may be petrogenetically linked and could also be linked to the other major groups of meteorites, nakhlites and chassignites. Although we do not know the field context for meteorites and have not constrained source craters, we can constrain their emplacement at or near the surface of Mars.

However, we currently only have 252 samples to understand an entire planet. All martian meteorites, except the polymict breccia NWA 7034 and the singular ALH 84001, have Amazonian ages, representing a biased sampling of the martian crust (McSween et al., 2009; Walton et al., 2008). Martian surface rocks have a higher SiO_2, higher alkalis, and lower MgO and CaO contents relative to the martian meteorites (Filiberto, 2017; McSween et al., 2009). Note that through terrestrial analogue analyses, a new study by Berger et al. (2020) shows that the APXS instrument on board of *Spirit*, *Opportunity*, and *Curiosity* rovers overestimated Al and S and underestimated Mg due to matrix effects. The olivine-bearing basalts and soils at the martian surface might be more similar to the olivine-bearing meteorites than previously thought. Nevertheless, only one sample, called Bounce Rock found in Meridiani Planum at the martian surface, has the same composition as meteorites (Zipfel et al., 2011). This bias signifies that the geologic diversity of Mars is not fully represented by martian meteorites. Thus, various questions still remain regarding the geology and evolution of Mars:

- How variable in composition is the martian interior, including the crust and mantle?
- How did the magma ocean crystallize, and how diverse are mantle/crustal sources on Mars?
- How has magmatic behavior (fractional crystallization, assimilation, accumulation) evolved with time on Mars?
- How were volcanic rocks emplaced at the martian surface?
- What is the volatile content in the martian interior and how did it evolve?
- What types of alteration occurred and what are their extent at the martian surface?
- What was the history of the martian dynamo prior to its demise?

Although martian meteorites have helped to reveal the nature of these uncertainties, a different set of samples is needed. We thus propose a wish list of desired characteristics for martian samples, many of which are missing from the martian meteorites:

- *In situ* igneous samples showing diversity in composition, possibly petrogenetically linked (i.e., evolution) and/or representing crustal assimilation;
- Samples with diverse elemental and isotopic composition and mineralogy, which reflect various igneous processes and different mantle sources;

- Igneous rocks with diverse textures (quenched glass, coarse- and fine-grained rocks) representing different cooling rate, and thus different magmatic behaviors;
- Mantle or lower crust xenoliths;
- Pre-Noachian and early Noachian samples, including evolved rocks, and/or containing magnetic minerals (pyrrhotite, magnetite, common on Mars), or iron oxide minerals (hematite, goethite, and maghemite), which preserve a record of the now-dead dynamo;
- Pre-Noachian, Noachian, and Hesperian rocks with a high potential for geochronology;
- Samples that underwent low degrees of impact metamorphism;
- Sedimentary rocks of any kind.

Returned martian samples are not yet available. However, the Mars 2020 mission, which is planned for launch in July 2020, will cache ≥31 samples for return to Earth as early as 2031 (Clery & Voosen, 2019). The landing site for Mars 2020 is Jezero crater (Fig. 11). Rocks in Jezero crater show diverse lithologies with different mineralogies, textures, and representing time periods from the early Noachian to the Amazonian. Jezero crater is a 45-km diameter open-lake basin, containing two delta deposits with a likely early Noachian paleolake system dated between ~3.95 – 3.97 Ga (Fassett and Head, 2005; Ehlmann et al., 2008; Goudge et al., 2012; 2015). Igneous minerals and basaltic compositions with limited pervasive alteration are ubiquitous in the different units of Jezero crater, including olivine (3 – 12%), pyroxene (24 – 30%), and plagioclase (18 – 25 %), and even K-feldspar (1 – 7.5%) (Salvatore et al., 2018). The stratigraphy near the landing ellipse of Mars 2020, includes the Noachian crust, basin fill consisting mostly of olivine and Mg-carbonates with an age of 3.82 ± 0.07 Ga (Mid to Late Noachian), an 2.6 ± 0.5 Ga (early Amazonian or late Hesperian) mafic cap, and pitted cap could either be an impact melt or volcanic unit (Goudge et al., 2015; Goudge et al., 2012; Horgan et al., 2020; Mandon et al., 2020; Salvatore et al., 2018). We likely will not bring samples with all characteristics from the wish list from Jezero crater, but it is possible that we will discover some of them in new martian meteorites. Before the returned samples come back to Earth (not before 2031), we might expect to recover at least 100 meteorites, based on the current recovery rate (Fig. 2).

Returned samples from Mars would allow us to better constrain the compositions of the martian interior, including elucidating the diversity of geochemical reservoirs. The field context that Mars 2020 — a key advantage for these samples over the martian meteorites — will provide a higher resolution view of igneous and other geological processes. Returned samples would also allow important chronological context constraints. At the moment, crater counting on Mars assumes lunar crater calibration, but Jezero crater shows potential volcanic flows (Goudge et al., 2015) that can provide a calibration point to enable better definition of crater ages, and as a benefit, the late accretion flux to Mars.

The complementary study of returned samples and meteorites will help constrain the evolution from the Noachian to the Amazonian of the martian interior. Meteorites and samples will inform each other to help reveal the secrets of the Red planet.

Acknowledgements and data availability

We would like to thank A. I. Sheen and D. L. Laczniak for help with data compilation. Funding for this work is provided by NASA grants 80NSSC19K0537 and 80NSSC17K0477 (AU), and 80NSSC18K0333 (TJL). This is LPI contribution no. XXXX. LPI is operated by USRA under a cooperative agreement with the Science Mission Directorate of the National Aeronautics and Space Administration. All data were previously published.

References

Agee, C. B., Walton, E. L., Tschauner, O., & Herd, C. D. K. (2016). Shock effects in new martian olivine basalt Northwest Africa 10416: Distinct from shergottites but akin Northwest Africa 8159. *Lunar and Planetary Science Conference XLVII*, Abstract #1639.

Agee, C. B., Wilson, N. V., McCubbin, F. M., Ziegler, K., Polyak, V. J., Sharp, Z. D., et al. (2013). Unique Meteorite from Early Amazonian Mars: Water-Rich Basaltic Breccia Northwest Africa 7034. *Science*, *339*(6121), 780–785. https://doi.org/10.1126/science.1228858

Ali, A., Jabeen, I., Gregory, D., Verish, R., & Banerjee, N. R. (2016). New triple oxygen isotope data of bulk and separated fractions from SNC meteorites: Evidence for mantle homogeneity of Mars. *Meteoritics & Planetary Science*, *51*(5), 981–995. https://doi.org/10.1111/maps.12640

Amelin, Y. (2002). Lead Isotopic Ages of Chondrules and Calcium-Aluminum-Rich Inclusions. *Science*, *297*(5587), 1678–1683. https://doi.org/10.1126/science.1073950

Anders, E., Shearer, C. K., Papike, J. J., Bell, J. F., Clemett, S. J., Zare, R. N., et al. (1996). Evaluating the Evidence for Past Life on Mars. *Science*, *274*(5295), 2119–2125.

Armytage, R. M. G., Debaille, V., Brandon, A. D., & Agee, C. B. (2018). A complex history of silicate differentiation of Mars from Nd and Hf isotopes in crustal breccia NWA 7034. *Earth and Planetary Science Letters*, *502*, 274–283. https://doi.org/10.1016/j.epsl.2018.08.013

Artemieva, N., & Ivanov, B. (2004). Launch of martian meteorites in oblique impacts. *Icarus*, *171*(1), 84–101. https://doi.org/10.1016/j.icarus.2004.05.003

Balta, J. B., Sanborn, M., McSween, H. Y., & Wadhwa, M. (2013). Magmatic history and parental melt composition of olivine-phyric shergottite LAR 06319: Importance of magmatic degassing and olivine antecrysts in Martian magmatism. *Meteoritics & Planetary Science*, *48*(8), 1359–1382. https://doi.org/10.1111/maps.12140

Balta, J. B., Sanborn, M. E., Udry, A., Wadhwa, M., & Mcsween, H. Y. (2015). Petrology and trace element geochemistry of Tissint, the newest shergottite fall. *Meteoritics & Planetary Science*, *50*(1), 63–85. https://doi.org/10.1111/maps.12403

Balta, J. B., Sanborn, M. E., Mayne, R. G., Wadhwa, M., McSween, H. Y., & Crossley, S. D. (2017). Northwest Africa 5790: A previously unsampled portion of the upper part of the nakhlite pile. *Meteoritics & Planetary Science*, *52*(1), 36–59. https://doi.org/10.1111/maps.12744

Barnes, J. J., McCubbin, F. M., Santos, A. R., Day, J. M. D., Boyce, J. W., Schwenzer, S. P., et al. (2020). Multiple early-formed water reservoirs in the interior of Mars. *Nature Geoscience*. https://doi.org/10.1038/s41561-020-0552-y

Basu Sarbadhikari, A., Day, J. M. D., Liu, Y., Rumble, D., & Taylor, L. A. (2009). Petrogenesis of olivine-phyric shergottite Larkman Nunatak 06319: Implications for enriched components in martian basalts. *Geochimica et Cosmochimica Acta*, *73*(7), 2190–2214. https://doi.org/10.1016/j.gca.2009.01.012

Basu Sarbadhikari, A., Babu, E. V. S. S. K., & Vijaya Kumar, T. (2016). Chemical layering in the upper mantle of Mars: Evidence from olivine-hosted melt inclusions in Tissint. *Meteoritics & Planetary Science*, *17*, 1–17. https://doi.org/10.1111/maps.12790

Beard, B. L., Ludois, J. M., Lapen, T. J., & Johnson, C. M. (2013). Pre-4.0 billion year weathering on Mars constrained by Rb-Sr geochronology on meteorite ALH84001. *Earth and Planetary Science Letters*, *361*, 173–182. https://doi.org/10.1016/j.epsl.2012.10.021

Bellucci, J. J., Nemchin, A. A., Whitehouse, M. J., Humayun, M., Hewins, R., & Zanda, B.

(2015). Pb-isotopic evidence for an early, enriched crust on Mars. *Earth and Planetary Science Letters*, *410*, 34–41. https://doi.org/10.1016/j.epsl.2014.11.018

Bellucci, J. J., Nemchin, A. A., Whitehouse, M. J., Snape, J. F., Kielman, R. B., Bland, P. A., & Benedix, G. K. (2016). A Pb isotopic resolution to the Martian meteorite age paradox. *Earth and Planetary Science Letters*, *433*(2013), 241–248. https://doi.org/10.1016/j.epsl.2015.11.004

Bellucci, J. J., Nemchin, A. A., Whitehouse, M. J., Snape, J. F., Bland, P., Benedix, G. K., & Roszjar, J. (2018). Pb evolution in the Martian mantle. *Earth and Planetary Science Letters*, *485*(7711), 79–87. https://doi.org/10.1016/j.epsl.2017.12.039

Bellucci, J. J., Herd, C. D. K., Whitehouse, M. J., Nemchin, A. A., Kenny, G. G., & Merle, R. E. (2020). Insights into the chemical diversity of the martian mantle from the Pb isotope systematics of Northwest Africa 8159. *Chemical Geology*, *Accepted*.

Berger, J. A., Schmidt, M. E., Campbell, J. L., Flannigan, E. L., Gellert, R., Ming, W., & Morris, R. V. (2020). Particle Induced X-ray Emission spectrometry (PIXE) of Hawaiian volcanics: An analogue study to evaluate the APXS field analysis of geologic materials on Mars. *Icarus*, 113708. https://doi.org/10.1016/j.icarus.2020.113708

Berkley, J. L., Keil, K., & Prinz, M. (1980). Comparative petrology and origin of Governador Valadares and other nakhlites. In *Lunar Planet. Sci. Conf. XI. Lunar Planet. Inst., Houston.* (Vol. 11, pp. 1089–1102).

Bianco, T. A., Ito, G., Becker, J. M., & Garcia, M. O. (2005). Secondary Hawaiian volcanism formed by flexural arch decompression. *Geochemistry, Geophysics, Geosystems*, *6*(8), 1–24. https://doi.org/10.1029/2005GC000945

Bibring, J. P., Langevin, Y., Gendrin, A., Gondet, B., Poulet, F., Berthé, M., et al. (2005). Mars surface diversity as revealed by the OMEGA/Mars express observations. *Science*, *307*(5715), 1576–1581. https://doi.org/10.1126/science.1108806

Bland, P. A. (2001). Quantification of Meteorite Infall Rates from Accumulations in Deserts, and Meteorite Accumulations on Mars. In B. Peucker-Ehrenbrink & B. Schmitz (Eds.), *Accretion of Extraterrestrial Matter Throughout Earth's History* (pp. 267–303). Boston, MA: Springer US. https://doi.org/10.1007/978-1-4419-8694-8_15

Bogard, D. D., & Johnson, P. (1983). Martian Gases in an Antarctic Meteorite? *Science*, *221*(4611), 651–654. https://doi.org/10.1126/science.221.4611.651

Borg, L. E., Gaffney, A. M., & DePaolo, D. (2008). Preliminary Age of Martian Meteorite Northwest Africa 4468 and Its Relationship to the Other Incompatible-Element-enriched Shergottites. *39th Lunar and Planetary Science Conference*, #1851.

Borg, L. E., & Drake, M. J. (2005). A review of meteorite evidence for the timing of magmatism and of surface or near-surface liquid water on Mars. *Journal of Geophysical Research*, *110*(E12), E12S03. https://doi.org/10.1029/2005JE002402

Borg, L. E., & Draper, D. S. (2003). A petrogenetic model for the origin and compositional variation of the martian basaltic meteorites. *Meteoritics & Planetary Science*, *38*(12), 1713–1731. https://doi.org/10.1111/j.1945-5100.2003.tb00011.x

Borg, L. E., Nyquist, L. E., Wiesmann, H., & Reese, Y. (2002). Constraints on the petrogenesis of Martian meteorites from the Rb-Sr and Sm-Nd isotopic systematics of the lherzolitic shergottites ALH77005 and LEW88516. *Geochimica et Cosmochimica Acta*, *66*(11), 2037–2053. https://doi.org/10.1016/S0016-7037(02)00835-9

Borg, L. E., Nyquist, L. E., Wiesmann, G., Shih, C. Y., & Reese, Y. (2003). The age of Dar al Gani 476 and the differentation history of the martian meteorites inferred from their radiogenic isotopic systematics. *Geochimica et Cosmochimica Acta*, *67*(18), 3519–3536. https://doi.org/10.1016/S0016-7037(03)00094-2

Borg, L. E., Brennecka, G. A., & Symes, S. J. K. (2016). Accretion timescale and impact history of Mars deduced from the isotopic systematics of martian meteorites.

Geochimica et Cosmochimica Acta, *175*, 150–167. https://doi.org/10.1016/j.gca.2015.12.002

Borg, Lars E., Connelly, J. N., Nyquist, L. E., Shih, C.-Y., Wiesmann, H., & Reese, Y. (1999). The Age of the Carbonates in Martian Meteorite ALH84001. *Science*, *286*(5437), 90–94. https://doi.org/10.1126/science.286.5437.90

Bouvier, A., Blichert-Toft, J., Vervoort, J. D., Gillet, P., & Albarède, F. (2008). The case for old basaltic shergottites. *Earth and Planetary Science Letters*, *266*(1–2), 105–124. https://doi.org/10.1016/j.epsl.2007.11.006

Bouvier, A., Blichert-Toft, J., & Albarède, F. (2009). Martian meteorite chronology and the evolution of the interior of Mars. *Earth and Planetary Science Letters*, *280*(1–4), 285–295. https://doi.org/10.1016/j.epsl.2009.01.042

Bouvier, L. C., Costa, M. M., Connelly, J. N., Jensen, N. K., Wielandt, D., Storey, M., et al. (2018). Evidence for extremely rapid magma ocean crystallization and crust formation on Mars. *Nature*, *558*(7711), 586–589. https://doi.org/10.1038/s41586-018-0222-z

Bowling, T. J., Johnson, B. C., Wiggins, S. E., Walton, E. L., Melosh, H. J., & Sharp, T. G. (2020). Dwell time at high pressure of meteorites during impact ejection from Mars. *Icarus*, 113689. https://doi.org/10.1016/j.icarus.2020.113689

Bradley, J. P. (1996). Magnetite whiskers and platelets in the ALH84001 Martian Evidence of vapor phase growth meteorite, *60*(24), 5149–5155.

Brandon, A. D., Puchtel, I. S., Walker, R. J., Day, J. M. D., Irving, A. J., & Taylor, L. A. (2012). Evolution of the martian mantle inferred from the 187Re–187Os isotope and highly siderophile element abundance systematics of shergottite meteorites. *Geochimica et Cosmochimica Acta*, *76*, 206–235. https://doi.org/10.1016/j.gca.2011.09.047

Brennecka, G. a., Borg, L. E., & Wadhwa, M. (2014). Insights into the Martian mantle: The age and isotopics of the meteorite fall Tissint. *Meteoritics & Planetary Science*, *49*(3), 412–418. https://doi.org/10.1111/maps.12258

Bridges, J. C., & Grady, M. M. (1999). A halite-siderite-anhydrite-chlorapatite assemblage in-Nakhla: Mineralogical evidence for evaporites on Mars. *Meteoritics & Planetary Science*, *34*(3), 407–415. https://doi.org/10.1111/j.1945-5100.1999.tb01349.x

Bridges, J. C., & Schwenzer, S. P. (2012). The nakhlite hydrothermal brine on Mars. *Earth and Planetary Science Letters*, *359–360*, 117–123. https://doi.org/10.1016/j.epsl.2012.09.044

Bridges, J. C., Catling, D. C., Saxton, J. M., Swindle, T. D., Lyon, I. C., & Grady, M. M. (2001). Alteration assemblages in Martian meteorites: Implications for near-surface processes. *Space Science Reviews*, *96*(1–4), 365–392. https://doi.org/10.1023/A:1011965826553

Bridges, J. C., Hicks, L. J., Bedford, C., & Macarthur, S. P. S. J. (2017). Igneous Differentiation of the Martian Crust, 764904. https://doi.org/10.1111/maps.1295.

Cannon, K. M., Mustard, J. F., & Agee, C. B. (2015). Evidence for a widespread basaltic breccia component in the martian low-albedo regions from the reflectance spectrum of Northwest Africa 7034. *Icarus*, *252*, 150–153. https://doi.org/10.1016/j.icarus.2015.01.016

Carlson, R. W., & Boyet, M. (2009). Short-lived radionuclides as monitors of early crust-mantle differentiation on the terrestrial planets. *Earth and Planetary Science Letters*, *279*(3–4), 147–156. https://doi.org/10.1016/j.epsl.2009.01.017

Caro, G., Bourdon, B., Halliday, A. N., & Quitté, G. (2008). Super-chondritic Sm/Nd ratios in Mars, the Earth and the Moon. *Nature*, *452*(7185), 336–339. https://doi.org/10.1038/nature06760

Carr, M. H., & Head, J. W. (2010). Geologic history of Mars. *Earth and Planetary Science Letters*, *294*(3–4), 185–203. https://doi.org/10.1016/j.epsl.2009.06.042

1298 Cassata, W. S., Cohen, B. E., Mark, D. F., Trappitsch, R., Crow, C. A., Wimpenny, J., et al.
1299 (2018). Chronology of martian breccia NWA 7034 and the formation of the martian
1300 crustal dichotomy. *Science Advances*, *4*(5). https://doi.org/10.1126/sciadv.aap8306
1301 Castle, N., & Herd, C. D. K. (2017). Experimental petrology of the Tissint meteorite: Redox
1302 estimates, crystallization curves, and evaluation of petrogenetic models. *Meteoritics &*
1303 *Planetary Science*, *52*(1), 125–146. https://doi.org/10.1111/maps.12739
1304 Castle, N., & Herd, C. D. K. (2018). Experimental investigation into the effects of oxidation
1305 during petrogenesis of the Tissint meteorite. *Meteoritics & Planetary Science*, *23*, 1–23.
1306 https://doi.org/10.1111/maps.13083
1307 Changela, H. G., & Bridges, J. C. (2010). Alteration assemblages in the nakhlites: Variation
1308 with depth on Mars. *Meteoritics & Planetary Science*, *45*(12), 1847–1867.
1309 https://doi.org/10.1111/j.1945-5100.2010.01123.x
1310 Chen, Y., Liu, Y., Guan, Y., Eiler, J. M., Ma, C., Rossman, G. R., & Taylor, L. A. (2015).
1311 Evidence in Tissint for recent subsurface water on Mars. *Earth and Planetary Science*
1312 *Letters*, *425*, 55–63. https://doi.org/10.1016/j.epsl.2015.05.004
1313 Clery, D., & Voosen, P. (2019). Bold plan to retrieve Mars samples takes shape. *Science*,
1314 *366*(6468), 932–933. https://doi.org/10.1126/science.366.6468.932
1315 Cohen, B. E., Mark, D. F., Cassata, W. S., Lee, M. R., Tomkinson, T., & Smith, C. L. (2017).
1316 Taking the pulse of Mars via dating of a plume-fed volcano. *Nature Communications*,
1317 *8*(1), 640. https://doi.org/10.1038/s41467-017-00513-8
1318 Combs, L. M., Udry, A., Howarth, G. H., Righter, M., Lapen, T. J., Gross, J., et al. (2019).
1319 Petrology of the enriched poikilitic shergottite Northwest Africa 10169: Insight into the
1320 martian interior. *Geochimica et Cosmochimica Acta*, *266*, 435–462.
1321 https://doi.org/10.1016/j.gca.2019.07.001
1322 Connelly, J. N., Bollard, J., & Bizzarro, M. (2017). Pb–Pb chronometry and the early Solar
1323 System. *Geochimica et Cosmochimica Acta*, *201*, 345–363.
1324 https://doi.org/10.1016/j.gca.2016.10.044
1325 Connelly, J. N, Bizzarro, M., Krot, A. N., Nordlund, A., Wielandt, D., & Ivanova, M. A.
1326 (2012). The Absolute Chronology and Thermal Processing of Solids in the Solar
1327 Protoplanetary Disk. *Science*, *338*(6107), 651–655.
1328 https://doi.org/10.1126/science.1226919
1329 Corrigan, C. M., Velbel, M. A., & Vicenzi, E. P. (2015). Modal abundances of pyroxene,
1330 olivine, and mesostasis in nakhlites: Heterogeneity, variation, and implications for
1331 nakhlite emplacement. *Meteoritics & Planetary Science*, *50*(9), 1497–1511.
1332 https://doi.org/10.1111/maps.12492
1333 Crozaz, G., Floss, C., & Wadhwa, M. (2003). Chemical alteration and REE mobilization in
1334 meteorites from hot and cold deserts. *Geochimica et Cosmochimica Acta*, *67*(24), 4727–
1335 4741. https://doi.org/10.1016/j.gca.2003.08.008
1336 Daly, L., Lee, M. R., Piazolo, S., Griffin, S., Bazargan, M., Campanale, F., et al. (2019).
1337 Boom boom pow: Shock-facilitated aqueous alteration and evidence for two shock
1338 events in the Martian nakhlite meteorites. *Science Advances*, *5*(9), eaaw5549.
1339 https://doi.org/10.1126/sciadv.aaw5549
1340 Daly, L., Piazolo, S., Lee, M. R., Griffin, S., Chung, P., Campanale, F., et al. (2019).
1341 Understanding the emplacement of Martian volcanic rocks using petrofabrics of the
1342 nakhlite meteorites. *Earth and Planetary Science Letters*, *520*, 220–230.
1343 https://doi.org/10.1016/j.epsl.2019.05.050
1344 Dann, J. C., Holzheid, A. H., Grove, T. L., & Mcsween, H. Y. (2001). Phase equilibria of the
1345 Shergotty meteorite: Constraints on pre-eruptive water contents of martian magmas and
1346 fractional crystallization under hydrous conditions. *Meteoritics & Planetary Science*,
1347 *36*(6), 793–806. https://doi.org/10.1111/j.1945-5100.2001.tb01917.x

Danyushevsky, L. V., Della-Pasqua, F. N., & Sokolov, S. (2000). Re-equilibration of melt inclusions trapped by magnesian olivine phenocrysts from subduction-related magmas: petrological implications. *Contributions to Mineralogy and Petrology*, *138*(1), 68–83. https://doi.org/10.1007/PL00007664

Dauphas, N., & Pourmand, A. (2011). Hf-W-Th evidence for rapid growth of Mars and its status as a planetary embryo. *Nature*, *473*(7348), 489–492. https://doi.org/10.1038/nature10077

Day, J. M. D., Tait, K. T., Udry, A., Moynier, F., Liu, Y., & Neal, C. R. (2018). Rejuvenated Magmatism on Mars. In *Lunar and Planetary Science Conference* (Vol. 49).

Day, J. M. D., Taylor, L. A., Floss, C., & McSween, H. Y. (2006). Petrology and chemistry of MIL 03346 and its significance in understanding the petrogenesis of nakhlites on Mars. *Meteoritics & Planetary Science*, *41*(4), 581–606. https://doi.org/10.1111/j.1945-5100.2006.tb00484.x

Day, J. M. D., Tait, K. T., Udry, A., Moynier, F., Liu, Y., & Neal, C. R. (2018). Martian magmatism from plume metasomatized mantle. *Nature Communications*, *9*(1), 4799. https://doi.org/10.1038/s41467-018-07191-0

Debaille, V., Yin, Q. Z., Brandon, A. D., & Jacobsen, B. (2008). Martian mantle mineralogy investigated by the 176Lu-176Hf and 147Sm-143Nd systematics of shergottites. *Earth and Planetary Science Letters*, *269*(1–2), 186–199. https://doi.org/10.1016/j.epsl.2008.02.008

Debaille, V., Brandon, A. D., Yin, Q. Z., & Jacobsen, B. (2007). Coupled 142Nd-143Nd evidence for a protracted magma ocean in Mars. *Nature*, *450*(7169), 525–528. https://doi.org/10.1038/nature06317

Debaille, V., Brandon, A. D., O'Neill, C., Yin, Q. Z., & Jacobsen, B. (2009). Early martian mantle overturn inferred from isotopic composition of nakhlite meteorites. *Nature Geoscience*, *2*(8), 548–552. https://doi.org/10.1038/ngeo579

Dreibus, G., & Wanke, H. (1985). Mars, a volatile-rich planet. *Meteoritics*, *20*, 367–381.

Dunham, E. T., Balta, J. B., Wadhwa, M., Sharp, T. G., & McSween, H. Y. (2019). Petrology and geochemistry of olivine-phyric shergottites LAR 12095 and LAR 12240: Implications for their petrogenetic history on Mars. *Meteoritics & Planetary Science*, *25*, 1–25. https://doi.org/10.1111/maps.13262

Ehlmann, B. L., Mustard, J. F., Fassett, C. I., Schon, S. C., Head, J. W., Des Marais, D. J., et al. (2008). Clay minerals in delta deposits and organic preservation potential on Mars. *Nature Geoscience*, *1*(6), 355–358. https://doi.org/10.1038/ngeo207

Elkins-Tanton, L. T. (2005). Possible formation of ancient crust on Mars through magma ocean processes. *Journal of Geophysical Research*, *110*(E12), E12S01. https://doi.org/10.1029/2005JE002480

Elkins-Tanton, L. T., Parmentier, E. M., & Hess, P. C. (2003). Magma ocean fractional crystallization and cumulate overturn in terrestrial planets: Implications for Mars. *Meteoritics & Planetary Science*, *38*(12), 1753–1771. https://doi.org/10.1111/j.1945-5100.2003.tb00013.x

Eugster, O., Busemann, H., Lorenzetti, S., & Terribilini, D. (2002). Ejection ages from krypton-81-krypton-83 dating and pre-atmospheric sizes of martian meteorites. *Meteoritics & Planetary Science*, *37*(10), 1345–1360. https://doi.org/10.1111/j.1945-5100.2002.tb01033.x

Fassett, C. I., & Head, J. W. (2005). Fluvial sedimentary deposits on Mars: Ancient deltas in a crater lake in the Nili Fossae region. *Geophysical Research Letters*, *32*(14), 1–5. https://doi.org/10.1029/2005GL023456

Ferdous, J., Brandon, A. D., Peslier, A. H., & Pirotte, Z. (2017). Evaluating crustal contributions to enriched shergottites from the petrology, trace elements, and Rb-Sr and

Sm-Nd isotope systematics of Northwest Africa 856. *Geochimica et Cosmochimica Acta*, *211*, 280–306. https://doi.org/10.1016/j.gca.2017.05.032
Filiberto, J. (2017). Geochemistry of Martian basalts with constraints on magma genesis. *Chemical Geology*, *466*, 1–14. https://doi.org/10.1016/j.chemgeo.2017.06.009
Filiberto, J., & Treiman, A. H. (2009). Martian magmas contained abundant chlorine, but little water. *Geology*, *37*(12), 1087–1090. https://doi.org/10.1130/G30488A.1
Filiberto, J., Musselwhite, D. S., Gross, J., Burgess, K., Le, L., & Treiman, A. H. (2010). Experimental petrology, crystallization history, and parental magma characteristics of olivine-phyric shergottite NWA 1068: Implications for the petrogenesis of "enriched" olivine-phyric shergottites. *Meteoritics & Planetary Science*, *45*(8), 1258–1270. https://doi.org/10.1111/j.1945-5100.2010.01080.x
Filiberto, J., Chin, E., Day, J. M. D., Franchi, I. a., Greenwood, R. C., Gross, J., et al. (2012). Geochemistry of intermediate olivine-phyric shergottite Northwest Africa 6234, with similarities to basaltic shergottite Northwest Africa 480 and olivine-phyric shergottite Northwest Africa 2990. *Meteoritics & Planetary Science*, *47*(8), 1256–1273. https://doi.org/10.1111/j.1945-5100.2012.01382.x
Filiberto, J., Gross, J., Trela, J., & Ferré, E. C. (2014). Gabbroic shergottite Northwest Africa 6963: An intrusive sample of Mars. *American Mineralogist*, *99*(4), 601–606. https://doi.org/10.2138/am.2014.4638
Filiberto, J., Treiman, A. H., Giesting, P. a., Goodrich, C. a., & Gross, J. (2014). High-temperature chlorine-rich fluid in the martian crust: A precursor to habitability. *Earth and Planetary Science Letters*, *401*, 110–115. https://doi.org/10.1016/j.epsl.2014.06.003
Filiberto, J., Baratoux, D., Beaty, D., Breuer, D., Farcy, B. J., Grott, M., et al. (2016). A review of volatiles in the Martian interior. *Meteoritics & Planetary Science*, *51*(11), 1935–1958. https://doi.org/10.1111/maps.12680
Filiberto, J., Gross, J., & McCubbin, F. M. (2016). Constraints on the water, chlorine, and fluorine content of the Martian mantle. *Meteoritics & Planetary Science*, *13*, 1–13. https://doi.org/10.1111/maps.12624
Filiberto, J., Gross, J., Udry, A., Trela, J., Wittmann, A., Cannon, K. M., et al. (2018). Shergottite Northwest Africa 6963: A Pyroxene-Cumulate Martian Gabbro. *Journal of Geophysical Research: Planets*, *123*(7), 1823–1841. https://doi.org/10.1029/2018JE005635
Filiberto, J., McCubbin, F. M., & Taylor, G. J. (2019). Volatiles in martian magmas and the interior: Inputs of volatiles into the crust and atmosphere. In *Volatiles in the Martian crust* (pp. 13–33). Elsevier.
Foley, C. N., Wadhwa, M., Borg, L. E., Janney, P. E., Hines, R., & Grove, T. L. (2005). The early differentiation history of Mars from 182W-142Nd isotope systematics in the SNC meteorites. *Geochimica et Cosmochimica Acta*, *69*(18), 4557–4571. https://doi.org/10.1016/j.gca.2005.05.009
Franz, H. B., Kim, S. T., Farquhar, J., Day, J. M. D., Economos, R. C., McKeegan, K. D., et al. (2014). Isotopic links between atmospheric chemistry and the deep sulphur cycle on Mars. *Nature*, *508*(7496), 364–368. https://doi.org/10.1038/nature13175
Fritz, J., Artemieva, N., & Greshake, A. (2005). Ejection of Martian meteorites. *Meteoritics & Planetary Science*, *40*(9–10), 1393–1411. https://doi.org/10.1111/j.1945-5100.2005.tb00409.x
Gaetani, G. A., O'Leary, J. A., Shimizu, N., Bucholz, C. E., & Newville, M. (2012). Rapid reequilibration of H 2O and oxygen fugacity in olivine-hosted melt inclusions. *Geology*, *40*(10), 915–918. https://doi.org/10.1130/G32992.1
Gaffney, A. M., Borg, L. E., Asmerom, Y., Shearer, C. K., & Burger, P. V. (2011). Disturbance of isotope systematics during experimental shock and thermal

metamorphism of a lunar basalt with implications for Martian meteorite chronology. *Meteoritics & Planetary Science*, *46*(1), 35–52. https://doi.org/10.1111/j.1945-5100.2010.01137.x

Genova, A., & Al., E. (2016). Seasonal and static gravity field of Mars from MGS, Mars Odyssey and MRO radio science. *Icarus*, *272*, 228–245.

Giesting, P. A., & Filiberto, J. (2014). Quantitative models linking igneous amphibole composition with magma Cl and OH content. *American Mineralogist*, *99*(4), 852–865. https://doi.org/10.2138/am.2014.4623

Giesting, P. A., & Filiberto, J. (2016). The formation environment of potassic-chloro-hastingsite in the nakhlites MIL 03346 and pairs and NWA 5790: Insights from terrestrial chloro-amphibole. *Meteoritics & Planetary Science*, *51*(11), 2127–2153. https://doi.org/10.1111/maps.12675

Giesting, P. A., Schwenzer, S. P., Filiberto, J., Starkey, N. A., Franchi, I. A., Treiman, A. H., et al. (2015). Igneous and shock processes affecting chassignite amphibole evaluated using chlorine/water partitioning and hydrogen isotopes. *Meteoritics & Planetary Science*, *50*(3), 433–460. https://doi.org/10.1111/maps.12430

Gillet, P., Barrat, J. a., Deloule, E., Wadhwa, M., Jambon, a., Sautter, V., et al. (2002). Aqueous alteration in the Northwest Africa 817 (NWA 817) Martian meteorite. *Earth and Planetary Science Letters*, *203*(1), 431–444. https://doi.org/10.1016/S0012-821X(02)00835-X

Goderis, S., Brandon, A. D., Mayer, B., & Humayun, M. (2016). Ancient impactor components preserved and reworked in martian regolith breccia Northwest Africa 7034. *Geochimica et Cosmochimica Acta*, *191*, 203–215. https://doi.org/10.1016/j.gca.2016.07.024

Goodrich, C. A. (2002). Olivine-phyric martian basalts: A new type of shergottite. *Meteoritics & Planetary Science*, *37*(S12), B31–B34. https://doi.org/10.1111/j.1945-5100.2002.tb00901.x

Goodrich, C. A., Treiman, A. H., Filiberto, J., Gross, J., & Jercinovic, M. (2013). K2O-rich trapped melt in olivine in the Nakhla meteorite: Implications for petrogenesis of nakhlites and evolution of the Martian mantle. *Meteoritics & Planetary Science*, *48*(12), 2371–2405. https://doi.org/10.1111/maps.12226

El Goresy, A., Gillet, P., Miyahara, M., Ohtani, E., Ozawa, S., Beck, P., & Montagnac, G. (2013). Shock-induced deformation of Shergottites: Shock-pressures and perturbations of magmatic ages on Mars. *Geochimica et Cosmochimica Acta*, *101*, 233–262. https://doi.org/10.1016/j.gca.2012.10.002

Goudge, T. A., Head, J. W., Mustard, J. F., & Fassett, C. I. (2012). An analysis of open-basin lake deposits on Mars: Evidence for the nature of associated lacustrine deposits and post-lacustrine modification processes. *Icarus*, *219*(1), 211–229. https://doi.org/10.1016/j.icarus.2012.02.027

Goudge, T. A., Mustard, J. F., Head, J. W., Fassett, C. I., & Wiseman, S. M. (2015). Assessing the mineralogy of the watershed and fan deposits of the Jezero crater paleolake system, Mars. *Journal of Geophysical Research: Planets*, *120*(4), 775–808. https://doi.org/10.1002/2014JE004782

Griffin, S., Daly, L., Lee, M. R., Piazolo, S., Trimby, P. W., Forman, L., et al. (2019). New insights into the magmatic and shock history of the nakhlite meteorites from electron backscatter diffraction. In *Lunar and Planetary Institute Science Conference L* (p. Abstract#1845).

Gross, J., Treiman, A. H., Filiberto, J., & Herd, C. D. K. (2011). Primitive olivine-phyric shergottite NWA 5789: Petrography, mineral chemistry, and cooling history imply a magma similar to Yamato-980459. *Meteoritics & Planetary Science*, *46*(1), 116–133.

https://doi.org/10.1111/j.1945-5100.2010.01152.x
Gross, J., Filiberto, J., Herd, C. D. K., Daswani, M. M., Schwenzer, S. P., & Treiman, A. H. (2013). Petrography, mineral chemistry, and crystallization history of olivine-phyric shergottite NWA 6234: A new melt composition. *Meteoritics & Planetary Science*, *48*(5), 854–871. https://doi.org/10.1111/maps.12092
Guitreau, M., & Flahaut, J. (2019). Record of low-temperature aqueous alteration of Martian zircon during the late Amazonian. *Nature Communications*, *10*(1), 2457. https://doi.org/10.1038/s41467-019-10382-y
Halevy, I., Fischer, W. W., & Eiler, J. M. (2011). Carbonates in the Martian meteorite Allan Hills 84001 formed at 18 ± 4 °C in a near-surface aqueous environment. *Proceedings of the National Academy of Sciences of the United States of America*, *108*(41), 16895–16899. https://doi.org/10.1073/pnas.1109444108
Hallis, L., & Taylor, G. (2011). Hydrogen Isotopes in the Nakhlites: Magmatic and Atmospheric Martian Reserviors Versus Terrestrial Contamination. *Meteoritics & Planetary Science*, *12*, 1787–1803.
Hallis, L. J., Ishii, H. A., Bradley, J. P., & Taylor, G. J. (2014). Transmission electron microscope analyses of alteration phases in martian meteorite MIL 090032. *Geochimica et Cosmochimica Acta*, *134*, 275–288. https://doi.org/10.1016/j.gca.2014.02.007
Hamilton, J. S., Herd, C. D. K., Walton, E. L., & Tornabene, L. L. (2020). Prioritizing candidtae source craters for martian meteorites. *Lunar and Planetary Institute Science Conference LI*, Abstract #2607.
Hamilton, V. E., Christensen, P. R., McSween, H. Y., & Bandfield, J. L. (2003). Searching for the source regions of martian meteorites using MGS TES: Integrating martian meteorites into the global distribution of igneous materials on Mars. *Meteoritics & Planetary Science*, *38*(6), 871–885. https://doi.org/10.1111/j.1945-5100.2003.tb00284.x
Hartmann, W., & Neukum, G. (2001). Cratering Chronology and the Evolution of Mars. *Space Science Reviews*, *96*(1), 165–194. https://doi.org/10.1023/A:1011945222010
Hawthorne, F. C. (1983). The crystal chemistry of the amphiboles. *The Canadian Mineralogist*, *21*, 173–480.
He, Q., Xiao, L., Balta, J. B., Baziotis, I. P., Hsu, W., & Guan, Y. (2015). Petrography and geochemistry of the enriched basaltic shergottite Northwest Africa 2975. *Meteoritics & Planetary Science*, *21*, 1–21. https://doi.org/10.1111/maps.12571
Head, J. N. (2002). Martian Meteorite Launch: High-Speed Ejecta from Small Craters. *Science*, *298*(5599), 1752–1756. https://doi.org/10.1126/science.1077483
Herd, C. D. K. (2003). The oxygen fugacity of olivine-phyric martian basalts and the components within the mantle and crust of Mars. *Meteoritics & Planetary Science*, *38*(12), 1793–1805. https://doi.org/10.1111/j.1945-5100.2003.tb00015.x
Herd, C. D. K. (2008). Basalts as Probes of Planetary Interior Redox State. *Reviews in Mineralogy and Geochemistry*, *68*(1), 527–553. https://doi.org/10.2138/rmg.2008.68.19
Herd, C. D. K. (2019). Reconciling redox: making spatrial and temporal sense of oxygen fugacity variations in martian igneous rocks. In *Lunar and Planetary Institute Science Conference L* (Abstract #2746).
Herd, C. D. K., Tornabene, L. L., Bowling, T. J., Walton, E. L., Sharp, T. G., & Melosh, H. J. (2017). New insights into source craters for the martian meteorites. *80th Annual Meeting of the Meteoritical Society*, *2017*(1987), #6334.
Herd, C. D. K., Tornabene, L. L., Bowling, T. J., Walton, E. K., Sharp, T. G., Melosh, H. J., et al. (2018). Linking martian meteorites to their source craters: New insights. In *Lunar and Planetary Institute Science Conference XLIX* (p. Abstract #2266).
Herd, C. D. K., Walton, E. L., Agee, C. B., Muttik, N., Ziegler, K., Shearer, C. K., et al. (2017). The Northwest Africa 8159 martian meteorite: Expanding the martian sample

suite to the early Amazonian. *Geochimica et Cosmochimica Acta*, *218*, 1–26. https://doi.org/10.1016/j.gca.2017.08.037

Herd, C. D. K, Borg, L. E., Jones, J. H., & Papike, J. J. (2002). Oxygen fugacity and geochemical variations in the martian basalts: implications for martian basalt petrogenesis and the oxidation state of the upper mantle of Mars. *Geochimica et Cosmochimica Acta*, *66*(11), 2025–2036. https://doi.org/10.1016/S0016-7037(02)00828-1

Herd, C. D. K., Treiman, A. H., McKay, G. A., & Shearer, C. K. (2005). Light lithophile elements in martian basalts: Evaluating the evidence for magmatic water degassing. *Geochimica et Cosmochimica Acta*, *69*(9), 2431–2440. https://doi.org/10.1016/j.gca.2004.10.030

Herzog, G. F., & Caffee, M. W. (2014). Cosmic-ray exposure ages of meteorites. *Meteorites and Cosmochemical Processes*, 419–454.

Hewins, R. H., Zanda, B., Humayun, M., Nemchin, A., Lorand, J. P., Pont, S., et al. (2017). Regolith breccia Northwest Africa 7533: Mineralogy and petrology with implications for early Mars. *Meteoritics & Planetary Science*, *52*(1), 89–124. https://doi.org/10.1111/maps.12740

Hewins, R. H., Zanda, B., Pont, S., & Zanetta, P. -M. (2019). Northwest Africa 10414, a pigeonite cumulate shergottite. *Meteoritics & Planetary Science*, *54*(9), 2132–2148. https://doi.org/10.1111/maps.13374

Horgan, B. H. N., Anderson, R. B., Dromart, G., Amador, E. S., & Rice, M. S. (2020). The mineral diversity of Jezero crater: Evidence for possible lacustrine carbonates on Mars. *Icarus*, *339*, 113526. https://doi.org/10.1016/j.icarus.2019.113526

Howarth, G. H., Pernet-Fisher, J. F., Balta, J. B., Barry, P. H., Bodnar, R. J., & Taylor, L. A. (2014). Two-stage polybaric formation of the new enriched, pyroxene-oikocrystic, lherzolitic shergottite, NWA 7397. *Meteoritics & Planetary Science*, *49*(10), 1812–1830. https://doi.org/10.1111/maps.12357

Howarth, G. H., Pernet-Fisher, J. F., Bodnar, R. J., & Taylor, L. A. (2015). Evidence for the exsolution of Cl-rich fluids in martian magmas: Apatite petrogenesis in the enriched lherzolitic shergottite Northwest Africa 7755. *Geochimica et Cosmochimica Acta*, *166*, 234–248. https://doi.org/10.1016/j.gca.2015.06.031

Howarth, G. H., & Udry, A. (2017). Trace elements in olivine and the petrogenesis of the intermediate, olivine-phyric shergottite NWA 10170. *Meteoritics & Planetary Science*, *52*(2), 391–409. https://doi.org/10.1111/maps.12799

Howarth, G. H., Udry, A., & Day, J. M. D. (2018). Petrogenesis of basaltic shergottite Northwest Africa 8657: Implications for fO2 correlations and element redistribution during shock melting in shergottites. *Meteoritics & Planetary Science*, *53*(2), 249–267. https://doi.org/10.1111/maps.12999

Hu, S., Lin, Y., Zhang, J., Hao, J., Yamaguchi, A., Zhang, T., et al. (2020). Volatiles in the martian crust and mantle: Clues from the NWA 6162 shergottite. *Earth and Planetary Science Letters*, *530*, 115902. https://doi.org/10.1016/j.epsl.2019.115902

Hui, H., Peslier, A. H., Lapen, T. J., Shafer, J. T., Brandon, A. D., & Irving, A. J. (2011). Petrogenesis of basaltic shergottite Northwest Africa 5298: Closed-system crystallization of an oxidized mafic melt. *Meteoritics & Planetary Science*, *46*(9), 1313–1328. https://doi.org/10.1111/j.1945-5100.2011.01231.x

Humayun, M., Nemchin, a, Zanda, B., Hewins, R. H., Grange, M., Kennedy, a, et al. (2013). Origin and age of the earliest Martian crust from meteorite NWA 7533. *Nature*, *503*(7477), 513–6. https://doi.org/10.1038/nature12764

Ikeda, Y., Kimura, M., Takeda, H., Shimoda, G., Kita, N. T., Morishita, Y., et al. (2006). Petrology of a new basaltic shergottite: Dhofar 378. *Antarctic Meteorite Research*, *19*,

20–44.
IMOST. (2018). The Potential Science and Engineering Value of Samples Delivered to Earth by Mars Sample Return, (co-chairs D. W. Beaty, M. M. Grady, H. Y. McSween, E. Sefton-Nash; documentarian B.L. Carrier; plus 66 co-authors), 186. In *white paper* (p. 186).
Izawa, M. R. M., Tait, K. T., Moser, D. E., Barker, I. R., Hyde, B. C., Nicklin, I., & Lapen, T. J. (2015). Mineralogy, petrology and geochronoly of intermediate shergottite NWA 7042. In *Lunar and Planetary Institute Science Conference XLVI* (p. Abstract #2523).
Jambon, A., Barrat, J. A., Bollinger, C., Sautter, V., Boudouma, O., Greenwood, R. C., et al. (2010). Northwest Africa 5790. Top Sequence of the Nakhlite Pile. In *Lunar and Planetary Institute Science Conference XLI* (p. Abstract #1696).
Jambon, A., Sautter, V., Barrat, J.-A., Gattacceca, J., Rochette, P., Boudouma, O., et al. (2016). Northwest Africa 5790: Revisiting nakhlite petrogenesis. *Geochimica et Cosmochimica Acta*, *190*(January), 191–212. https://doi.org/10.1016/j.gca.2016.06.032
Jones, J. H. (1986). A discussion of isotopic systematics and mineral zoning in the shergottites: Evidence for a 180 m.y. igneous crystallization age. *Geochimica et Cosmochimica Acta*, *50*(6), 969–977. https://doi.org/10.1016/0016-7037(86)90377-7
Jones, J. H. (1989). Isotopic relationships among the shergottites, the nakhlites and Chassigny. In *Lunar and Planetary Science Conference Proceedings* (Vol. 19, pp. 465–474).
Kereszturi, A., & Chatzitheodoridis, E. (2016). Searching for the Source Crater of Nakhlite Meteorites. *Origins of Life and Evolution of Biospheres*, *46*(4), 455–471. https://doi.org/10.1007/s11084-016-9498-x
Kiefer, W. S. (2003). Melting in the martian mantle: Shergottite formation and implications for present-day mantle convection on Mars. *Meteoritics & Planetary Science*, *38*(12), 1815–1832. https://doi.org/10.1111/j.1945-5100.2003.tb00017.x
Kizovski, T. V, Tait, K. T., Cecco, V. E. D. I., White, L. F., & Moser, D. E. (2019). Detailed mineralogy and petrology of highly shocked poikilitic shergottite Northwest Africa 6342, *17*, 1–17. https://doi.org/10.1111/maps.13255
Kleine, T., Mezger, K., Münker, C., Palme, H., & Bischoff, A. (2004). 182Hf-182W isotope systematics of chondrites, eucrites, and martian meteorites: Chronology of core formation and early mantle differentiation in Vesta and Mars. *Geochimica et Cosmochimica Acta*, *68*(13), 2935–2946. https://doi.org/10.1016/j.gca.2004.01.009
Koike, M., Nakada, R., Kajitani, I., Usui, T., Tamenori, Y., Sugahara, H., & Kobayashi, A. (2020). In-situ preservation of nitrogen-bearing organics in Noachian Martian carbonates. *Nature Communications*, *11*(1), 1–7. https://doi.org/10.1038/s41467-020-15931-4
Kring, D. A., Gleason, J. D., Swindle, T. D., Nishiizumi, K., Caffee, M. W., Hill, D. H., et al. (2003). Composition of the first bulk melt sample from a volcanic region of Mars: Queen Alexandra Range 94201. *Meteoritics & Planetary Science*, *38*(12), 1833–1848. https://doi.org/10.1111/j.1945-5100.2003.tb00018.x
Kruijer, T. S., Kleine, T., Borg, L. E., Brennecka, G. A., Irving, A. J., Bischoff, A., & Agee, C. B. (2017). The early differentiation of Mars inferred from Hf–W chronometry. *Earth and Planetary Science Letters*, *474*, 345–354. https://doi.org/10.1016/j.epsl.2017.06.047
Kuchka, C. R., Herd, C. D. K., Walton, E. L., Guan, Y., & Liu, Y. (2017). Martian low-temperature alteration materials in shock-melt pockets in Tissint: Constraints on their preservation in shergottite meteorites. *Geochimica et Cosmochimica Acta*, *210*, 228–246. https://doi.org/10.1016/j.gca.2017.04.037
Kuebler, K. E. (2013). A comparison of the iddingsite alteration products in two terrestrial basalts and the Allan Hills 77005 martian meteorite using Raman spectroscopy and

electron microprobe analyses. *Journal of Geophysical Research : Planets*, *118*(4), 803–830. https://doi.org/10.1029/2012JE004243

Lang, N. P., Tornabene, L. L., McSween, H. Y., & Christensen, P. R. (2009). Tharsis-sourced relatively dust-free lavas and their possible relationship to Martian meteorites. *Journal of Volcanology and Geothermal Research*, *185*(1–2), 103–115. https://doi.org/10.1016/j.jvolgeores.2008.12.014

Lapen, T. J., Righter, M., Brandon, a D., Beard, B. L., Shafer, J., & Irving, A. J. (2009). Lu-Hf isotope systematics of NWA 4468 and NWA 2990; implications for the sources of shergottites. In *40th Lunar and Planetary Science Conference* (p. Abstract# 2376).

Lapen, T. J., Righter, M., Brandon, A. D., Debaille, V., Beard, B. L., Shafer, J. T., & Peslier, A. H. (2010). A Younger Age for ALH84001 and Its Geochemical Link to Shergottite Sources in Mars. *Science*, *328*(5976), 347–351. https://doi.org/10.1126/science.1185395

Lapen, T. J., Righter, M., Andreasen, R., Irving, A. J., Satkoski, A. M., Beard, B. L., et al. (2017). Two billion years of magmatism recorded from a single Mars meteorite ejection site. *Science Advances*, *3*(2), e1600922. https://doi.org/10.1126/sciadv.1600922

Lee, M. R., Cohen, B. E., Hallis, L. J., Boyce, A., & Mark, D. F. (2018). Aqueous alteration of the Martian meteorite Northwest Africa 817 : Probing fluid – rock interaction at the nakhlite launch site, *2412*(11), 2395–2412. https://doi.org/10.1111/maps.13136

Lentz, R. C. F., McSween, H. Y., Ryan, J., & Riciputi, L. R. (2001). Water in martian magmas: Clues from light lithophile elements in shergottite and nakhlite pyroxenes. *Geochimica et Cosmochimica Acta*, *65*(24), 4551–4565. https://doi.org/10.1016/S0016-7037(01)00756-6

Leshin, L. A. (2000). Insights into martian water reservoirs from analyses of martian meteorite QUE94201. *Geophysical Research Letters*, *27*(14), 2017–2020. https://doi.org/10.1029/1999GL008455

Leshin, L. A, & Vicenzi, E. (2006). Aqueous Processes Recorded by Martian Meteorites: Analyzing Martian Water on Earth. *Elements*, *2*, 157–162.

Leshin, Laurie A., Epstein, S., & Stolper, E. M. (1996). Hydrogen isotope geochemistry of SNC meteorites. *Geochimica et Cosmochimica Acta*, *60*(14), 2635–2650. https://doi.org/10.1016/0016-7037(96)00122-6

Liu, Y., Baziotis, I. P., Asimow, P. D., Bodnar, R. J., & Taylor, L. A. (2016). Mineral chemistry of the Tissint meteorite: Indications of two-stage crystallization in a closed system. *Meteoritics & Planetary Science*, *23*, 1–23. https://doi.org/10.1111/maps.12726

Liu, Y., Ma, C., Beckett, J. R., Chen, Y., & Guan, Y. (2016). Rare-earth-element minerals in martian breccia meteorites NWA 7034 and 7533: Implications for fluid–rock interaction in the martian crust. *Earth and Planetary Science Letters*, *451*(12), 251–262. https://doi.org/10.1016/j.epsl.2016.06.041

Liu, Y., Chen, Y., Guan, Y., Ma, C., Rossman, G. R., Eiler, J. M., & Zhang, Y. (2018). Impact-melt hygrometer for Mars: The case of shergottite Elephant Moraine (EETA) 79001. *Earth and Planetary Science Letters*, *490*, 206–215. https://doi.org/10.1016/j.epsl.2018.03.019

Lorand, J. P., Hewins, R. H., Humayun, M., Remusat, L., Zanda, B., La, C., & Pont, S. (2018). Chalcophile-siderophile element systematics of hydrothermal pyrite from martian regolith breccia NWA 7533. *Geochimica et Cosmochimica Acta*, *241*, 134–149. https://doi.org/10.1016/j.gca.2018.08.041

Mandon, L., Quantin-Nataf, C., Thollot, P., Mangold, N., Lozac'h, L., Dromart, G., et al. (2020). Refining the age, emplacement and alteration scenarios of the olivine-rich unit in the Nili Fossae region, Mars. *Icarus*, *336*, 113436. https://doi.org/10.1016/j.icarus.2019.113436

Mari, N., Riches, A. J. V., Hallis, L. J., Marrocchi, Y., Villeneuve, J., Gleissner, P., et al.

(2019). Syneruptive incorporation of martian surface sulphur in the nakhlite lava flows revealed by S and Os isotopes and highly siderophile elements: implication for mantle sources in Mars. *Geochimica et Cosmochimica Acta*. https://doi.org/10.1016/j.gca.2019.05.025

McCubbin, F. M., Hauri, E. H., Elardo, S. M., Vander Kaaden, K. E., Wang, J., & Shearer, C. K. (2012). Hydrous melting of the martian mantle produced both depleted and enriched shergottites. *Geology*, *40*(8), 683–686. https://doi.org/10.1130/G33242.1

McCubbin, F. M., Elardo, S. M., Shearer, C. K., Smirnov, A., Hauri, E. H., & Draper, D. S. (2013). A petrogenetic model for the comagmatic origin of chassignites and nakhlites: Inferences from chlorine-rich minerals, petrology, and geochemistry. *Meteoritics & Planetary Science*, *48*(5), 819–853. https://doi.org/10.1111/maps.12095

McCubbin, F. M., Boyce, J. W., Novák-Szabó, T., Santos, A. R., Tartèse, R., Muttik, N., et al. (2016). Geologic history of Martian regolith breccia Northwest Africa 7034: Evidence for hydrothermal activity and lithologic diversity in the Martian crust. *Journal of Geophysical Research: Planets*, *121*(10), 2120–2149. https://doi.org/10.1002/2016JE005143

McCubbin, F. M., Boyce, J. W., Srinivasan, P., Santos, A. R., Elardo, S. M., Filiberto, J., et al. (2016). Heterogeneous distribution of H 2 O in the Martian interior: Implications for the abundance of H2O in depleted and enriched mantle sources. *Meteoritics & Planetary Science*, *51*(11), 2036–2060. https://doi.org/10.1111/maps.12639

McDonough, W. F., & Sun, S. S. (1995). The composition of the Earth. *Chemical Geology*, *120*(3–4), 223–253. https://doi.org/10.1016/0009-2541(94)00140-4

McKay, D. S., Gibson, E. K., Thomas-Keprta, K. L., Vali, H., Romanek, C. S., Clemett, S. J., et al. (1996). Search for past life on Mars: Possible relic biogenic activity in martian meteorite ALH84001. *Science*, *273*(5277), 924–930. https://doi.org/10.1126/science.273.5277.924

McSween, H. Y., Taylor, G. J., & Wyatt, M. B. (2009). Elemental Composition of the Martian Crust. *Science*, *324*(5928), 736–739. https://doi.org/10.1126/science.1165871

McSween, H. Y. (2015). Petrology on Mars. *American Mineralogist*, *100*(11–12), 2380–2395. https://doi.org/10.2138/am-2015-5257

McSween, H.Y. (2019). The Search for Biosignatures in Martian Meteorite Allan Hills 84001. In *Advances in Astrobiology and Biogeophysics* (pp. 167–182). https://doi.org/10.1007/978-3-319-96175-0_8

McSween, H.Y., Eisenhour, D. D., Taylor, L. A., Wadhwa, M., & Crozaz, G. (1996). QUE94201 shergottite: Crystallization of a Martian basaltic magma. *Geochimica et Cosmochimica Acta*, *60*(22), 4563–4569. https://doi.org/10.1016/S0016-7037(96)00265-7

McSween, H. Y, & Stolper, E. M. (1980). Basaltic Meteorites. *Scientific American*, *242*(6), 54–63.

McSween, H. Y., Grove, T. L., Lentz, R. C. F., Dann, J. C., Holzheid, A. H., Riciputi, L. R., & Ryan, J. G. (2001). Geochemical evidence for magmatic water within Mars from pyroxenes in the Shergotty meteorite. *Nature*, *409*(6819), 487–490. https://doi.org/10.1038/35054011

Médard, E., & Grove, T. L. (2008). The effect of H2O on the olivine liquidus of basaltic melts: Experiments and thermodynamic models. *Contributions to Mineralogy and Petrology*, *155*(4), 417–432. https://doi.org/10.1007/s00410-007-0250-4

Melwani Daswani, M., Schwenzer, S. P., Reed, M. H., Wright, I. P., & Grady, M. M. (2016). Alteration minerals, fluids, and gases on early Mars: Predictions from 1-D flow geochemical modeling of mineral assemblages in meteorite ALH 84001. *Meteoritics & Planetary Science*, *51*(11), 2154–2174. https://doi.org/10.1111/maps.12713

Mikouchi, T, Makishima, J., & Kurihara, T. (2012). Relative Burial Depth of Nakhlites Revisited. In *Lunar and Planetary Institute Science Conference XLIII* (p. Abstract #2363).

Mikouchi, Takashi, & Kurihara, T. (2008). Mineralogy and petrology of paired lherzolitic shergottites Yamato 000027, Yamato 000047, and Yamato 000097: Another fragment from a Martian "lherzolite" block. *Polar Science*, *2*(3), 175–194. https://doi.org/10.1016/j.polar.2008.06.003

Mittlefehldt, D. W. (1994). ALH84001, a cumulate orthopyroxenite member of the martian meteorite clan. *Meteoritics*, *29*(2), 214–221. https://doi.org/10.1111/j.1945-5100.1994.tb00673.x

Moriwaki, R., Usui, T., Tobita, M., & Yokoyama, T. (2020). Geochemically heterogeneous Martian mantle inferred from Pb isotope systematics of depleted shergottites. *Geochimica et Cosmochimica Acta*, *274*, 157–171. https://doi.org/10.1016/j.gca.2020.01.014

Moser, D. E., Chamberlain, K. R., Tait, K. T., Schmitt, a K., Darling, J. R., Barker, I. R., & Hyde, B. C. (2013). Solving the Martian meteorite age conundrum using micro-baddeleyite and launch-generated zircon. *Nature*, *499*(7459), 454–7. https://doi.org/10.1038/nature12341

Moser, D. E., Arcuri, G. A., Reinhard, D. A., White, L. F., Darling, J. R., Barker, I. R., et al. (2019). Decline of giant impacts on Mars by 4.48 billion years ago and an early opportunity for habitability. *Nature Geoscience*, *12*(7), 522–527. https://doi.org/10.1038/s41561-019-0380-0

Mouginis-Mark, P. J., McCoy, T. J., Taylor, G. J., & Keil, K. (1992). Martian parent craters for the SNC meteorites. *Journal of Geophysical Research: Planets*, *97*(E6), 10213–10225.

Nekvasil, H, Dondolini, a, Horn, J., Filiberto, J., Long, H., & Lindsley, D. H. (2004). The Origin and Evolution of Silica-saturated Alkalic Suites: an Experimental Study. *Journal of Petrology*, *45*(4), 693–721. https://doi.org/10.1093/petrology/egg103

Nekvasil, H., Filiberto, J., McCubbin, F. M., & Lindsley, D. H. (2007). Alkalic parental magmas for chassignites? *Meteoritics & Planetary Science*, *42*(6), 979–992. https://doi.org/10.1111/j.1945-5100.2007.tb01145.x

Nyquist, L. E., Bogard, D. D., Shih, C.-Y., Greshake, A., Stöffler, D., & Eugster, O. (2001). Ages and geologic histories of Martian meteorites. In *Chronology and evolution of Mars* (pp. 105–164). Springer.

Nyquist, L. E., Bogard, D. D., Shih, C.-Y., Park, J., Reese, Y. D., & Irving, A. J. (2009). Concordant Rb–Sr, Sm–Nd, and Ar–Ar ages for Northwest Africa 1460: A 346Ma old basaltic shergottite related to "lherzolitic" shergottites. *Geochimica et Cosmochimica Acta*, *73*(14), 4288–4309. https://doi.org/10.1016/j.gca.2009.04.008

Nyquist, L. E., Shih, C., McCubbin, F. M., Santos, A. R., Shearer, C. K., Peng, Z. X., et al. (2016). Rb-Sr and Sm-Nd isotopic and REE studies of igneous components in the bulk matrix domain of Martian breccia Northwest Africa 7034. *Meteoritics & Planetary Science*, *51*(3), 483–498. https://doi.org/10.1111/maps.12606

Ody, A., Poulet, F., Quantin, C., Bibring, J.-P., Bishop, J. L., & Dyar, M. D. (2015). Candidates source regions of martian meteorites as identified by OMEGA/MEx. *Icarus*, *258*, 366–383. https://doi.org/10.1016/j.icarus.2015.05.019

Ostwald, A. M., Udry, A., Gross, J., & Day, J. M. D. (2020). Chassignite and nakhlite parental melts determined from melt inclusion analysis. In *Lunar and Planetary Institute Science Conference LI* (p. Abstract #2213).

Papike, J. J., Burger, P. V., Shearer, C. K., & McCubbin, F. M. (2013). Experimental and crystal chemical study of the basalt-eclogite transition in Mars and implications for

martian magmatism. *Geochimica et Cosmochimica Acta*, *104*, 358–376. https://doi.org/10.1016/j.gca.2012.11.007

Peslier, A. H., Hnatyshin, D., Herd, C. D. K., Walton, E. L., Brandon, A. D., Lapen, T. J., & Shafer, J. T. (2010). Crystallization, melt inclusion, and redox history of a Martian meteorite: Olivine-phyric shergottite Larkman Nunatak 06319. *Geochimica et Cosmochimica Acta*, *74*(15), 4543–4576. https://doi.org/10.1016/j.gca.2010.05.002

Peslier, A. H., Hervig, R., Yang, S., Humayun, M., Barnes, J. J., Irving, A. J., & Brandon, A. D. (2019). Determination of the water content and D/H ratio of the martian mantle by unraveling degassing and crystallization effects in nakhlites. *Geochimica et Cosmochimica Acta*, *266*, 382–415. https://doi.org/10.1016/j.gca.2019.04.023

Peslier, A. H. (2010). A review of water contents of nominally anhydrous natural minerals in the mantles of Earth, Mars and the Moon. *Journal of Volcanology and Geothermal Research*, *197*(1–4), 239–258. https://doi.org/10.1016/j.jvolgeores.2009.10.006

Peters, T. J., Simon, J. I., Jones, J. H., Usui, T., Moriwaki, R., Economos, R. C., et al. (2015). Tracking the source of the enriched martian meteorites in olivine-hosted melt inclusions of two depleted shergottites, Yamato 980459 and Tissint. *Earth and Planetary Science Letters*, *418*, 91–102. https://doi.org/10.1016/j.epsl.2015.02.033

Piercy, J. D., Bridges, J. C., Hicks, L. J., MacArthur, J. L., Greenwood, R. C., & Franchi, I. A. (2020). Terrestrial Alteration Mineral Assemblages in the NWA 10416 Olivine Phyric Shergottite. *Geochimica et Cosmochimica Acta*. https://doi.org/10.1016/j.gca.2020.03.026

Rahib, R. R., Udry, A., Howarth, G. H., Gross, J., Paquet, M., Combs, L. M., et al. (2019). Mantle source to near-surface emplacement of enriched and intermediate poikilitic shergottites in Mars. *Geochimica et Cosmochimica Acta*, *266*, 463–496. https://doi.org/10.1016/j.gca.2019.07.034

Righter, M., Lapen, T. J., & Irving, A. J. (2018). Extending the range in ages and source compositions of shergottites: Lu-Hf and Sm-Nd ages and isotope systematics of Northwest Africa 4480. In *Lunar and Planetary Institute Science Conference XLIX* (p. Abstract #2609).

Rubin, A. E., Warren, P. H., Greenwood, J. P., Verish, R. S., Leshin, L. A., Hervig, R. L., et al. (2000). Los Angeles: The most differentiated basaltic martian meteorite. *Geology*, *28*(11), 1011–1014.

Salvatore, M. R., Goudge, T. A., Bramble, M. S., Edwards, C. S., Bandfield, J. L., Amador, E. S., et al. (2018). Bulk mineralogy of the NE Syrtis and Jezero crater regions of Mars derived through thermal infrared spectral analyses. *Icarus*, *301*, 76–96. https://doi.org/10.1016/j.icarus.2017.09.019

Sandwell, D. T., Müller, R. D., Smith, W. H. F., Garcia, E., & Francis, R. (2014). New global marine gravity model from \ CryoSat-2 and Jason-1 reveals buried tectonic structure. *Science*, *346*, 65–67.

Santos, A. R., Agee, C. B., McCubbin, F. M., Shearer, C. K., Burger, P. V, Tartèse, R., & Anand, M. (2015). Petrology of igneous clasts in Northwest Africa 7034: Implications for the petrologic diversity of the martian crust. *Geochimica et Cosmochimica Acta*, *157*, 56–85. https://doi.org/10.1016/j.gca.2015.02.023

Sautter, V., Jambon, A., & Boudouma, O. (2006). Cl-amphibole in the nakhlite MIL 03346: Evidence for sediment contamination in a Martian meteorite. *Earth and Planetary Science Letters*, *252*(1–2), 45–55. https://doi.org/10.1016/j.epsl.2006.09.024

Shafer, J. T., Brandon, a. D., Lapen, T. J., Righter, M., Peslier, a. H., & Beard, B. L. (2010). Trace element systematics and 147Sm-143Nd and 176Lu-176Hf ages of Larkman Nunatak 06319: Closed-system fractional crystallization of an enriched shergottite magma. *Geochimica et Cosmochimica Acta*, *74*(24), 7307–7328.

https://doi.org/10.1016/j.gca.2010.09.009
Sharp, T. G., Walton, E. L., Hu, J., & Agee, C. (2019). Shock conditions recorded in NWA 8159 martian augite basalt with implications for the impact cratering history on Mars. *Geochimica et Cosmochimica Acta*, *246*, 197–212. https://doi.org/10.1016/j.gca.2018.11.014
Shearer, C. K., Bell, A. S., Herd, C. D. K., Burger, P. V, Provencio, P., Sharp, Z. D., & Papike, J. J. (2019). The Northwest Africa 8159 (NWA 8159) Martian Meteorite Part 2. Spinel-orthopyroxene intergrowths. A record of fO2 and crust-basalt interactions. *Geochimica et Cosmochimica Acta*, *258*, 242–257. https://doi.org/10.1016/j.gca.2019.05.034
Shih, C. Y., Nyquist, L. E., Reese, Y., & Misawa, K. (2011). Sm-Nd and Rb-Sr studies of lherzolitic shergottite Yamato 984028. *Polar Science*, *4*(4), 515–529. https://doi.org/10.1016/j.polar.2010.05.004
Stoker, C. R., Gooding, J. L., Roush, T., Banin, A., Burt, D., Clark, B. C., et al. (1993). The physical and chemical properties and resource potential of Martian surface soils. *Rnes*, 659–707.
Stolper, E., & McSween, H. Y. (1979). Petrology and origin of the shergottite meteorites. *Geochimica et Cosmochimica Acta*, *43*(9), 1475–1498. https://doi.org/10.1016/0016-7037(79)90142-X
Stolper, E. M., Baker, M. B., Newcombe, M. E., Schmidt, M. E., Treiman, a. H., Cousin, A., et al. (2013). The Petrochemistry of Jake_M: A Martian Mugearite. *Science*, *341*(6153), 1239463–1239463. https://doi.org/10.1126/science.1239463
Symes, S. J. K., Borg, L. E., Shearer, C. K., & Irving, A. J. (2008). The age of the martian meteorite Northwest Africa 1195 and the differentiation history of the shergottites. *Geochimica et Cosmochimica Acta*, *72*(6), 1696–1710. https://doi.org/10.1016/j.gca.2007.12.022
Tait, K. T., & Day, J. M. D. (2018). Chondritic late accretion to Mars and the nature of shergottite reservoirs. *Earth and Planetary Science Letters*, *494*, 99–108. https://doi.org/10.1016/j.epsl.2018.04.040
Taylor, G. J. (2013). The bulk composition of Mars. *Chemie Der Erde*. Elsevier GmbH. https://doi.org/10.1016/j.chemer.2013.09.006
Thomas-Keprta, K. L., Bazylinski, D. A., Kirschvink, J. L., Clemett, S. J., McKay, D. S., Wentworth, S. J., et al. (2000). Elongated prismatic magnetite crystals in ALH84001 carbonate globules: Potential Martian magnetofossils. *Geochimica et Cosmochimica Acta*, *64*(23), 4049–4081. https://doi.org/10.1016/S0016-7037(00)00481-6
Tomkinson, T., Lee, M. R., Mark, D. F., Dobson, K. J., & Franchi, I. A. (2015). The Northwest Africa (NWA) 5790 meteorite: A mesostasis-rich nakhlite with little or no Martian aqueous alteration. *Meteoritics & Planetary Science*, *50*(2), 287–304. https://doi.org/10.1111/maps.12424
Tornabene, L. L., Moersch, J. E., McSween, H. Y., McEwen, A. S., Piatek, J. L., Milam, K. A., & Christensen, P. R. (2006). Identification of large (2-10 km) rayed craters on Mars in THEMIS thermal infrared images: Implications for possible Martian meteorite source regions. *Journal of Geophysical Research E: Planets*, *111*(10), 1–25. https://doi.org/10.1029/2005JE002600
Treiman, A. H. (1985). Amphibole and hercynite spinel in Shergotty and Zagami: Magmatic water, depth of crystallization, and metasotism. *Meteoritics*, *20*, 229–243.
Treiman, A. H. (2005). The nakhlite meteorites: Augite-rich igneous rocks from Mars. *Chemie Der Erde - Geochemistry*, *65*(3), 203–270. https://doi.org/10.1016/j.chemer.2005.01.004
Treiman, A. H. (2019). Meteorite Allan Hills (ALH) 84001: Implications for Mars'

1898 inhabitation and habitability. In *The First Billion Years: Habitability* (p. Abstract #1032).
1899 Treiman, A. H., Barrett, R. S., & Gooding, J. L. (1993). Preterrestrial aqueous alteration of
1900 the Lafyette (SNC) meteorite. *Meteoritics*, *28*, 86–97.
1901 Treiman, A. H. (1995). S ≠ NC: Multiple source areas for Martian meteorites. *Journal of*
1902 *Geophysical Research*, *100*(E3), 5329. https://doi.org/10.1029/94JE02184
1903 Treiman, Allan H. (1998). The history of Allan Hills 84001 revised: multiple shock events.
1904 *Meteoritics & Planetary Science*, *33*(4), 753–764. https://doi.org/10.1111/j.1945-
1905 5100.1998.tb01681.x
1906 Treiman, A. H., Musselwhite, D. S., Herd, C. D. K. K., & Shearer, C. K. (2006). Light
1907 lithophile elements in pyroxenes of Northwest Africa (NWA) 817 and other Martian
1908 meteorites: Implications for water in Martian magmas. *Geochimica et Cosmochimica*
1909 *Acta*, *70*(11), 2919–2934. https://doi.org/10.1016/j.gca.2006.03.008
1910 Treiman, Allan H. (2003). Submicron Magnetite Grains and Carbon Compounds in Martian
1911 Meteorite ALH84001: Inorganic, Abiotic Formation by Shock and Thermal
1912 Metamorphism. *Astrobiology*, *3*(2), 369–392.
1913 https://doi.org/10.1089/153110703769016451
1914 Treiman, A. H, & Filiberto, J. (2014). Geochemical diversity of shergottite basalts : Mixing
1915 and fractionation , and their relation to Mars surface basalts, *17*.
1916 https://doi.org/10.1111/maps.12363
1917 Treiman, A. H, Bish, D. L., Vaniman, D. T., Chipera, S. J., Blake, D. F., Ming, D. W., et al.
1918 (2016). Mineralogy, provenance, and diagenesis of a potassic basaltic sandstone on
1919 Mars: CheMin X-ray diffraction of the Windjana sample (Kimberley area, Gale Crater).
1920 *Journal of Geophysical Research: Planets*, *121*(1), 75–106.
1921 https://doi.org/10.1002/2015JE004932
1922 Udry, A., & Day, J. M. D. (2018). 1.34 billion-year-old magmatism on Mars evaluated from
1923 the co-genetic nakhlite and chassignite meteorites. *Geochimica et Cosmochimica Acta*,
1924 *238*, 292–315. https://doi.org/10.1016/j.gca.2018.07.006
1925 Udry, A., Balta, J. B., & McSween, H. Y. (2014). Exploring fractionation models for Martian
1926 magmas. *Journal of Geophysical Research: Planets*, *119*(1), 1–18.
1927 https://doi.org/10.1002/2013JE004445
1928 Udry, A., Howarth, G. H., Lapen, T. J., & Righter, M. (2017). Petrogenesis of the NWA 7320
1929 enriched martian gabbroic shergottite: Insight into the martian crust. *Geochimica et*
1930 *Cosmochimica Acta*, *204*(3), 1–18. https://doi.org/10.1016/j.gca.2017.01.032
1931 Udry, A., Lunning, N. G., McSween, H. Y., & Bodnar, R. J. (2014). Petrogenesis of a
1932 vitrophyre in the martian meteorite breccia NWA 7034. *Geochimica et Cosmochimica*
1933 *Acta*, *141*, 281–293. https://doi.org/10.1016/j.gca.2014.06.026
1934 Udry, A., McSween, H. Y., Hervig, R. L., & Taylor, L. A. (2016). Lithium isotopes and light
1935 lithophile element abundances in shergottites: Evidence for both magmatic degassing
1936 and subsolidus diffusion. *Meteoritics & Planetary Science*, *51*(1), 80–104.
1937 https://doi.org/10.1111/maps.12582
1938 Udry, A., Howarth, G. H., Lapen, T. J., & Righter, M. (2017). Petrogenesis of the NWA 7320
1939 enriched martian gabbroic shergottite: Insight into the martian crust. *Geochimica et*
1940 *Cosmochimica Acta*, *204*, 1–18. https://doi.org/10.1016/j.gca.2017.01.032
1941 Usui, T., Mcsween, H. Y., & Floss, C. (2009). Petrogenesis of olivine-phyric shergottite
1942 Yamato 980459 , revisited. *Geochimica et Cosmochimica Acta*, *72*(6), 1711–1730.
1943 https://doi.org/10.1016/j.gca.2008.01.011
1944 Usui, T., Sanborn, M., Wadhwa, M., & McSween, H. Y. (2010). Petrology and trace element
1945 geochemistry of Robert Massif 04261 and 04262 meteorites, the first examples of
1946 geochemically enriched lherzolitic shergottites. *Geochimica et Cosmochimica Acta*,
1947 *74*(24), 7283–7306. https://doi.org/10.1016/j.gca.2010.09.010

Usui, T., Alexander, C. M. O. D., Wang, J., Simon, J. I., & Jones, J. H. (2012). Origin of water and mantle–crust interactions on Mars inferred from hydrogen isotopes and volatile element abundances of olivine-hosted melt inclusions of primitive shergottites. *Earth and Planetary Science Letters*, *357–358*, 119–129. https://doi.org/10.1016/j.epsl.2012.09.008

Usui, T., Alexander, C. M. O. D., Wang, J., Simon, J. I., & Jones, J. H. (2015). Meteoritic evidence for a previously unrecognized hydrogen reservoir on Mars. *Earth and Planetary Science Letters*, *410*, 140–151. https://doi.org/10.1016/j.epsl.2014.11.022

Vaci, Z., Agee, C. B., Herd, C. D. K., Walton, E. L., Tschauauner, O., Ziegler, K., et al. (2020). Hydrous Olivine Alteration on Mars and Earth. Meteoritics & Planetary Science. *Meteoritics & Planetary Science*, (In Press).

Valley, J. W., Eiler, J. M., Graham, C. M., Gibson, E. K., Romanek, C. S., Stolper, E. M., et al. (1997). Low-Temperature Carbonate Concretions in the Martian Meteorite ALH84001 : Evidence from Stable Isotopes and Mineralogy. *Science*, *275*(5306), 1633–1638.

Velbel, M. A. (2012). Aqueous alteration in Martian meteorites: Comparing mineral relations in igneous-rock weathering of Martian meteorites and in the sedimentary cycle of Mars. *Sedimentary Geology of Mars*, (102), 97–117. https://doi.org/10.2110/pec.12.102.0097

Velbel, M. A. (2016). Aqueous corrosion of olivine in the Mars meteorite Miller Range (MIL) 03346 during Antarctic weathering: Implications for water on Mars. *Geochimica et Cosmochimica Acta*, *180*, 126–145. https://doi.org/10.1016/j.gca.2016.01.036

Villanueva, G. L., Mumma, M. J., Novak, R. E., Käufl, H. U., Hartogh, P., Encrenaz, T., et al. (2015). Strong water isotopic anomalies in the martian atmosphere: Probing current and ancient reservoirs. *Science*, *348*(6231), 218–221. https://doi.org/10.1126/science.aaa3630

Wadhwa, M. (2001). Redox state of Mars' upper mantle and crust from Eu anomalies in shergottite pyroxenes. *Science*, *291*(5508), 1527–1530. https://doi.org/10.1126/science.1057594

Wadhwa, M., & Crozaz, G. (1995). Trace and minor elements in minerals of nakhlites and Chassigny: Clues to their petrogenesis. *Geochimica et Cosmochimica Acta*, *59*(17), 3629–3645. https://doi.org/10.1016/0016-7037(95)00228-R

Wadhwa, M., McCoy, T. J., & Schrader, D. L. (2020). Advances in Cosmochemistry Enabled by Antarctic Meteorites. *Annual Review of Earth and Planetary Sciences*, *48*(1), annurev-earth-082719-055815. https://doi.org/10.1146/annurev-earth-082719-055815

Walton, E. L., Sharp, T. G., Hu, J., & Filiberto, J. (2014). Heterogeneous mineral assemblages in martian meteorite Tissint as a result of a recent small impact event on Mars. *Geochimica et Cosmochimica Acta*, *140*, 334–348. https://doi.org/10.1016/j.gca.2014.05.023

Walton, E. L., Irving, A. J., Bunch, T. E., & Herd, C. D. K. (2012). Northwest Africa 4797: A strongly shocked ultramafic poikilitic shergottite related to compositionally intermediate Martian meteorites. *Meteoritics & Planetary Science*, *47*(9), 1449–1474. https://doi.org/10.1111/j.1945-5100.2012.01407.x

Walton, E. L., Kelley, S. P., & Spray, J. G. (2007). Shock implantation of Martian atmospheric argon in four basaltic shergottites: A laser probe40Ar/39Ar investigation. *Geochimica et Cosmochimica Acta*, *71*(2), 497–520. https://doi.org/10.1016/j.gca.2006.09.004

Walton, Erin L., Kelley, S. P., & Herd, C. D. K. (2008). Isotopic and petrographic evidence for young Martian basalts. *Geochimica et Cosmochimica Acta*, *72*(23), 5819–5837. https://doi.org/10.1016/j.gca.2008.09.005

Wanke, H., & Dreibus, G. (1988). Chemical Composition and Accretion History of Terrestrial Planets. *Philosophical Transactions of the Royal Society A: Mathematical, Physical and*

1998 *Engineering Sciences*, *325*(1587), 545–557. https://doi.org/10.1098/rsta.1988.0067
1999 Wanke, H., Dreibus, G., & Wright, I. P. (1994). Chemistry and Accretion History of Mars
2000 [and Discussion]. *Philosophical Transactions of the Royal Society A: Mathematical,*
2001 *Physical and Engineering Sciences*, *349*(1690), 285–293.
2002 https://doi.org/10.1098/rsta.1994.0132
2003 Warren, P. H., Greenwood, J. P., & Rubin, a E. (2004). Los Angeles: A tale of two stones.
2004 *Meteoritics & Planetary Science*, *39*(1), 137–156. https://doi.org/10.1111/j.1945-
2005 5100.2004.tb00054.x
2006 Webster, C. R., Mahaffy, P. R., Flesch, G. J., Niles, P. B., Jones, J. H., Leshin, L. A., et al.
2007 (2013). Isotope Ratios of H, C, and O in CO2 and H2O of the Martian Atmosphere.
2008 *Science*, *341*(6143), 260–263. https://doi.org/10.1126/science.1237961
2009 Werner, S. C., Ody, A., & Poulet, F. (2014). The Source Crater of Martian Shergottite
2010 Meteorites. *Science*, *343*(6177), 1343–1346. https://doi.org/10.1126/science.1247282
2011 Wieler, R., Huber, L., Busemann, H., Seiler, S., Leya, I., Maden, C., et al. (2016). Noble
2012 gases in 18 Martian meteorites and angrite Northwest Africa 7812-Exposure ages,
2013 trapped gases, and a re-evaluation of the evidence for solar cosmic ray-produced neon in
2014 shergottites and other achondrites. *Meteoritics & Planetary Science*, *51*(2), 407–428.
2015 https://doi.org/10.1111/maps.12600
2016 Williams, J. T., Shearer, C. K., Sharp, Z. D., Burger, P. V., McCubbin, F. M., Santos, A. R.,
2017 et al. (2016). The chlorine isotopic composition of Martian meteorites 1: Chlorine
2018 isotope composition of Martian mantle and crustal reservoirs and their interactions.
2019 *Meteoritics & Planetary Science*, *19*, 1–19. https://doi.org/10.1111/maps.12647
2020 Wilson, L., & Head, J. W. (1981). Volcanic eruption mechanisms on Mars: some theoretical
2021 constraints. *Lunar and Planetary Institute*, 1194–1195.
2022 Wittmann, A., Korotev, R. L., Jolliff, B. L., Irving, A. J., Moser, D. E., Barker, I., & Rumble,
2023 D. (2015). Petrography and composition of Martian regolith breccia meteorite Northwest
2024 Africa 7475. *Meteoritics & Planetary Science*, *50*(2), 326–352.
2025 https://doi.org/10.1111/maps.12425
2026 Yoshizaki, T., & McDonough, W. F. (2020). The composition of Mars. *Geochimica et*
2027 *Cosmochimica Acta*, *273*, 137–162. https://doi.org/10.1016/J.GCA.2020.01.011
2028 Zipfel, J., Schröder, C., Jolliff, B. L., Gellert, R., Herkenhoff, K. E., Rieder, R., et al. (2011).
2029 Bounce Rock-A shergottite-like basalt encountered at Meridiani Planum, Mars.
2030 *Meteoritics & Planetary Science*, *46*(1), 1–20. https://doi.org/10.1111/j.1945-
2031 5100.2010.01127.x
2032

Figure captions

Figure 1. Schematic representing the different information that martian meteorites can provide about the martian surface and interior. Blue bubbles represent highly volatile compounds, such as OH, H_2O, CO_2, Cl, and S. Not at scale.

Figure 2. Number of meteorites recovered each year separated by types of martian meteorites (x-axis with no continuous years).

Figure 3. From top to bottom and left to right: Basaltic shergottites: NWA 8657 (BSE image); Olivine-phyric shergottite: LAR 06319 (XPL image); Poikilitic shergottite NWA 4468 (XPL image); Gabbroic shergottite NWA 6369 (BSE image); Augite-rich shergottite: NWA 8159 (BSE image from Herd et al., 2017); Regolith breccia NWA 7034 (BSE image); Nakhlite: MIL 090030 (XPL image); Chassignite: NWA 2737 (XPL image); Orthopyroxenite ALH 84001 (XPL image, from LPI Allan Treiman). Scale bars represent 500 μm for all images.

Figure 4. Calculated $^{176}Lu/^{177}Hf$ and $^{147}Sm/^{144}Nd$ mantle source ratios of shergottites and ALH 84001 (Red with 2SD error bars; Lapen et al., 2017 and references therein) are plotted with a superimposed hypothetical source end-member mixing array (gray) using end-member compositions (green) calculated from a progressive Mars magma ocean (MMO) crystallization model of Debaille et al. (2008). The enriched end-member, which is identical to the independently-calculated source composition for ALH 84001, is hypothesized to reflect residual trapped liquid in equilibrium with cumulates of upper mantle (UM1). The most depleted end-member can be represented by an assemblage that reflects earlier-formed cumulates formed during MMO crystallization (UM2). The third component could either be represented by cumulates forming UM1 or shallow upper mantle (SUM98). In the modeled mixing array (gray), it is assumed that SUM98 represents the upper mantle cumulate assemblage. Please see Debaille et al. (2008) and Lapen et al. (2010; 2017) for details of the MMO crystallization modeling and data.

Figure 5. Timeline of major processes in Mars' history based on martian meteorite studies (see text for references). Age periods from Hartmann & Neukum (2001) chronology. The most recent studies were used in this figure for each processes: a) references for crystallization ages in text; b) accretion and core formation from Foley (2005), Kruijer et al. (2017), Kleine et al. (2004); c) MMO crystallization from Kruijer et al. (2017); d) crust formation from Bouvier et al. (2018); e) shergottite source ages from Borg et al. (2016), Kruijer et al. (2017), Foley et al. (2005); f) nakhlite source age from Debaille et al. (2009); g) ALH 84001 source age from Kruijer et al. (2017); and h) NWA 7034 source ages from Kruijer et al. (2017) and Bouvier et al. (2018).

Figure 6. Interpretation of possible emplacement scenarios for a) olivine-phyric, b) poikilitic, and c) basaltic and gabbroic shergottites. See text for details. Note that the relative grain size of different mineral in the different types of shergottites are not at the same scale.

Figure 7. Epsilon $^{143}Nd_{(present\ day)}$ versus $\varepsilon^{142}Nd_{(measured)}$ for shergottites (Red) and nakhlites (Orange) (data from Debaille et al., 2007; 2009; Borg et al., 2016; Lapen et al., 2010;2017). Superimposed on the data are a modeled mixing line or isochron for shergottites (Green) and an isochron diagram (black and blue lines) assuming a chondritic uniform reservoir (CHUR) system bulk composition (blue star). The dashed gray curved lines reflect, from left-to-right,

$^{147}Sm/^{144}Nd$ ratios of 0.15, 0.17, 0.196 (CHUR), 0.23, 0.25, 0.28, and 0.30. The shergottite data form a linear array (Green line) that is both consistent with mixing between enriched and depleted end-members (e.g., Figure 4; Debaille et al., 2007) and as an isochron (e.g., Borg et al., 2016). If the data represents a mixing line and Mars has a Sm/Nd ratio of CHUR, the data would predict that the slope of the array has no age significance. However, since the end-member compositions reflect materials formed during MMO crystallization, the mixing line intercepts of the isochrons at their respective Sm/Nd ratios (dashed gray lines) would have age significance (e.g., Debaille et al., 2007). In this case, the modeled formation ages of the depleted and enriched end-member compositions would be about 4510 and 4400 Ma (blue), respectively. These dates are about 50 Ma younger than those calculated by Debaille et al. (2007) due to the more extended range in shergottite data since 2007. Of course, the dates are strongly model dependent, but the important prediction is that the depleted cumulates formed before the more enriched components, consistent with progressive MMO crystallization. If the shergottite data do have unique age significance and represent reservoirs that formed at exactly the same time, an apparent age of 4504 ± 6 Ma can be calculated. Whether the shergottite data represents a mixing line or an isochron, the nakhlite data (orange) indicate that they cannot be related to shergottite mantle sources and also indicate that Sm and Nd were decoupled in the nakhlite mantle source prior to nakhlite petrogenesis.

Figure 8. Schematic representing the emplacement of shergottite-like lavas versus nakhlite-lavas based on a lithospheric flexure model (from Day et al., 2018) and using a terrestrial analog from Hawaii (Bianco et al., 2005). The lithosphere above the plume is slightly thinner. Not at scale.

Figure 9. Different shergottite, nakhlite, chassignite, and NWA 7034 sources based on initial epsilon Nd and Sr/Sr bulk compositions, LREE enrichment for shergottites (modified after Day et al., 2018; Shearer et al., 2019 and NWA 7034 data from Agee et al., 2013).

Figure 10. Oxygen fugacity (fO_2, in log units, relative to the QFM buffer) of representative shergottites versus whole-rock La/Yb (CI-normalized). Oxygen fugacity data sources for olivine-phyric (early-crystallizing assemblages only) and basaltic shergottites as summarized in Castle & Herd (2017) and updated in Herd (2019), except for additional estimates, which are calculated using Fe-Ti oxide data from Ferdous et al. (2017), Hui et al. (2011), and Ikeda et al. (2006). Poikilitic shergottite data representing the early-crystallizing assemblages are from Rahib et al. (2019), Kizovski et al. (2019) and Walton et al. (2012). Exponential lines-of-best-fit are shown for each set of data: solid black line = poikilitic; dashed grey line = olivine-phyric; dashed black line = basaltic. The envelopes represent the three different enriched, intermediate, and depleted shergottite groups.

Figure 11. Mars topography map from Mars Orbiter Laser Altimeter (MOLA) instrument, including main martian regions and landing sites of successful NASA missions and their landing dates. The landing date of the NASA Mars 2020 rover is scheduled on February 18 2021 and the landing date of ESA ExoMars 2020 is not yet known.

2126 Figure 1

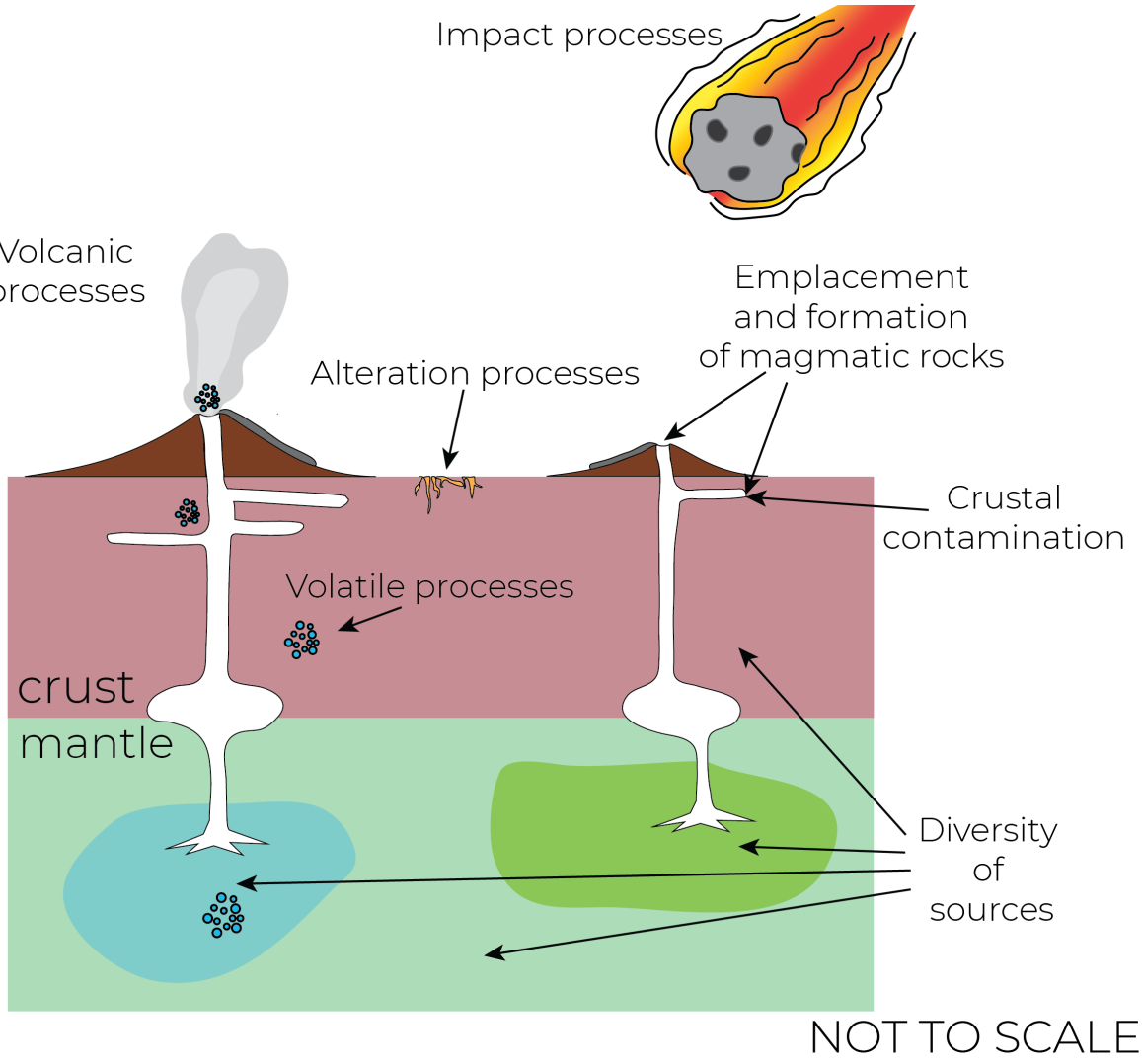

2127
2128

2129 Figure 2

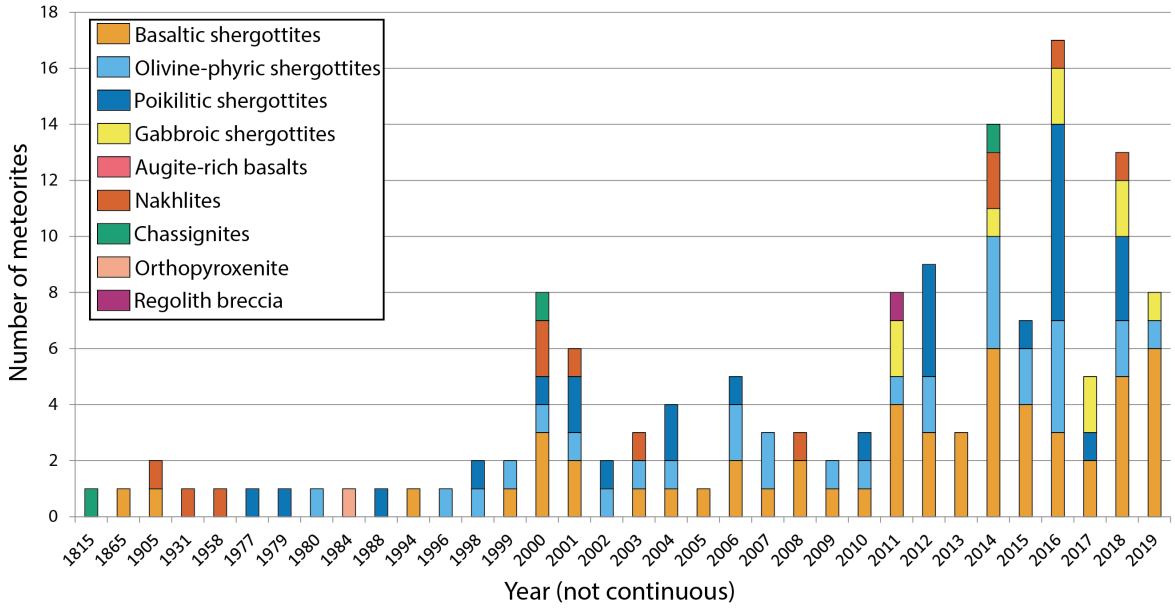

2130

2131 Figure 3

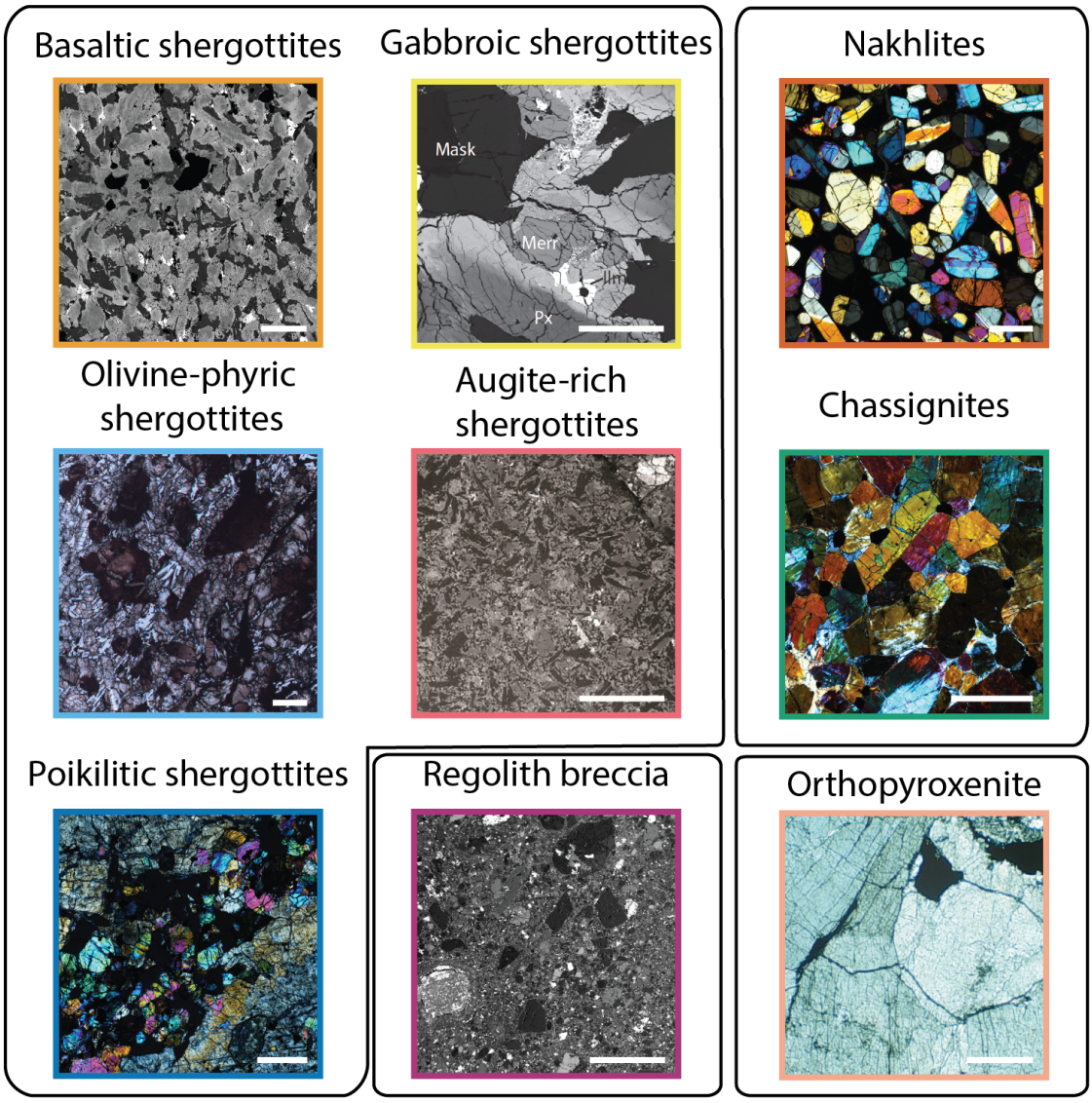

2132

2133 Figure 4

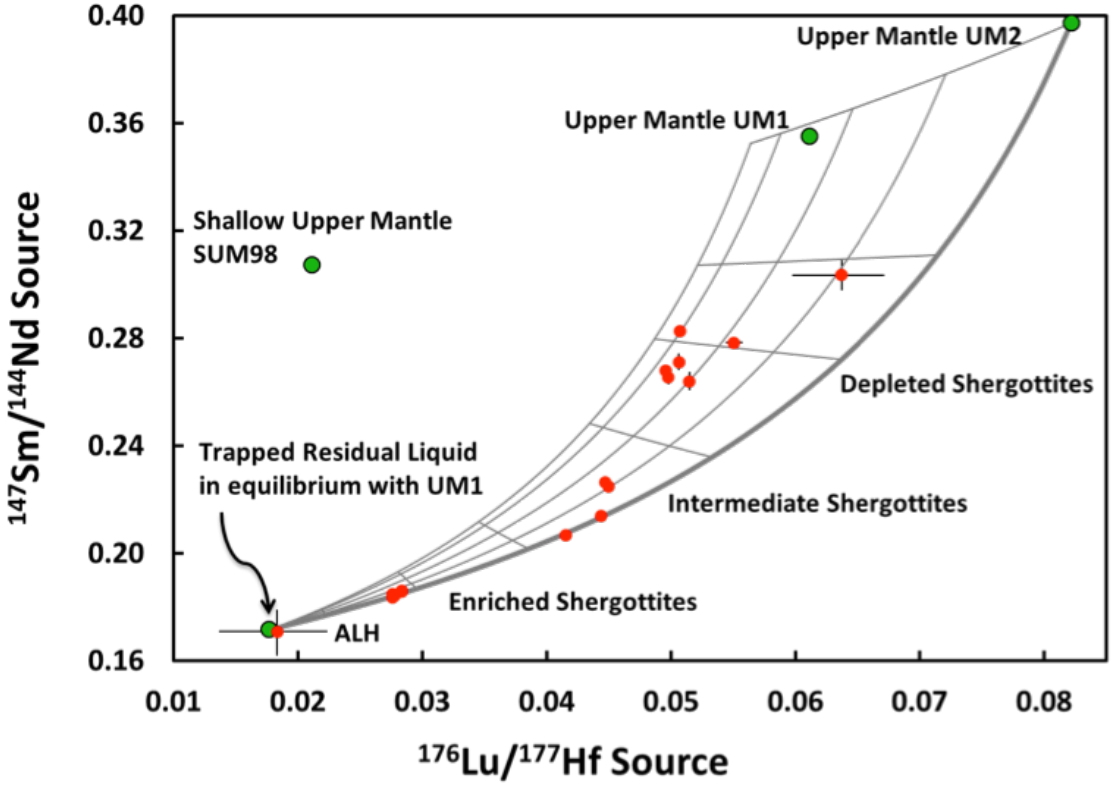

2134

2135 Figure 5
2136

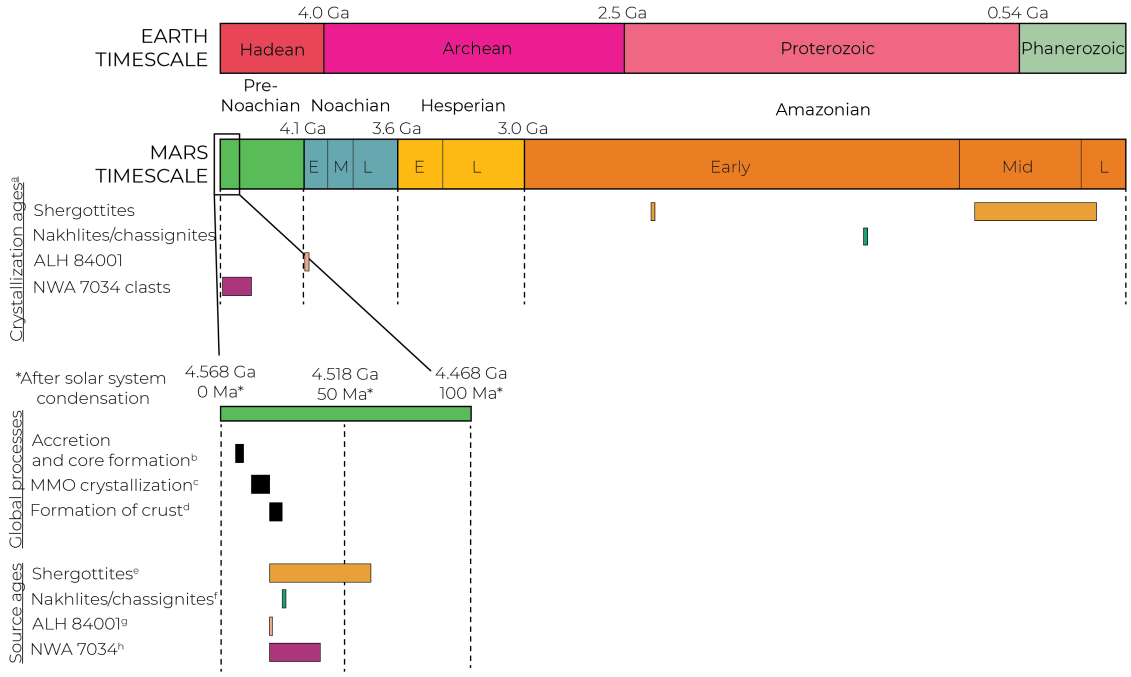

2137

2138 Figure 6

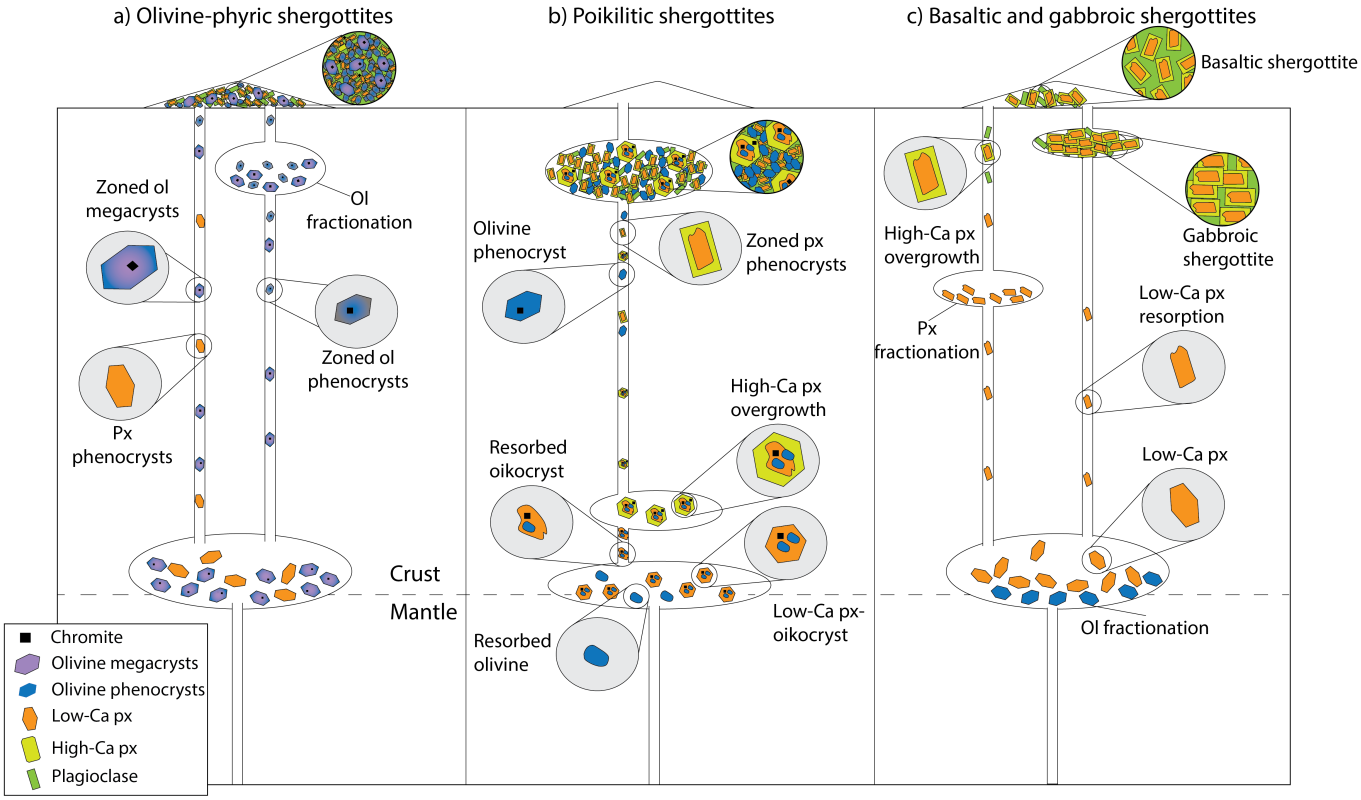

2139 Figure 7

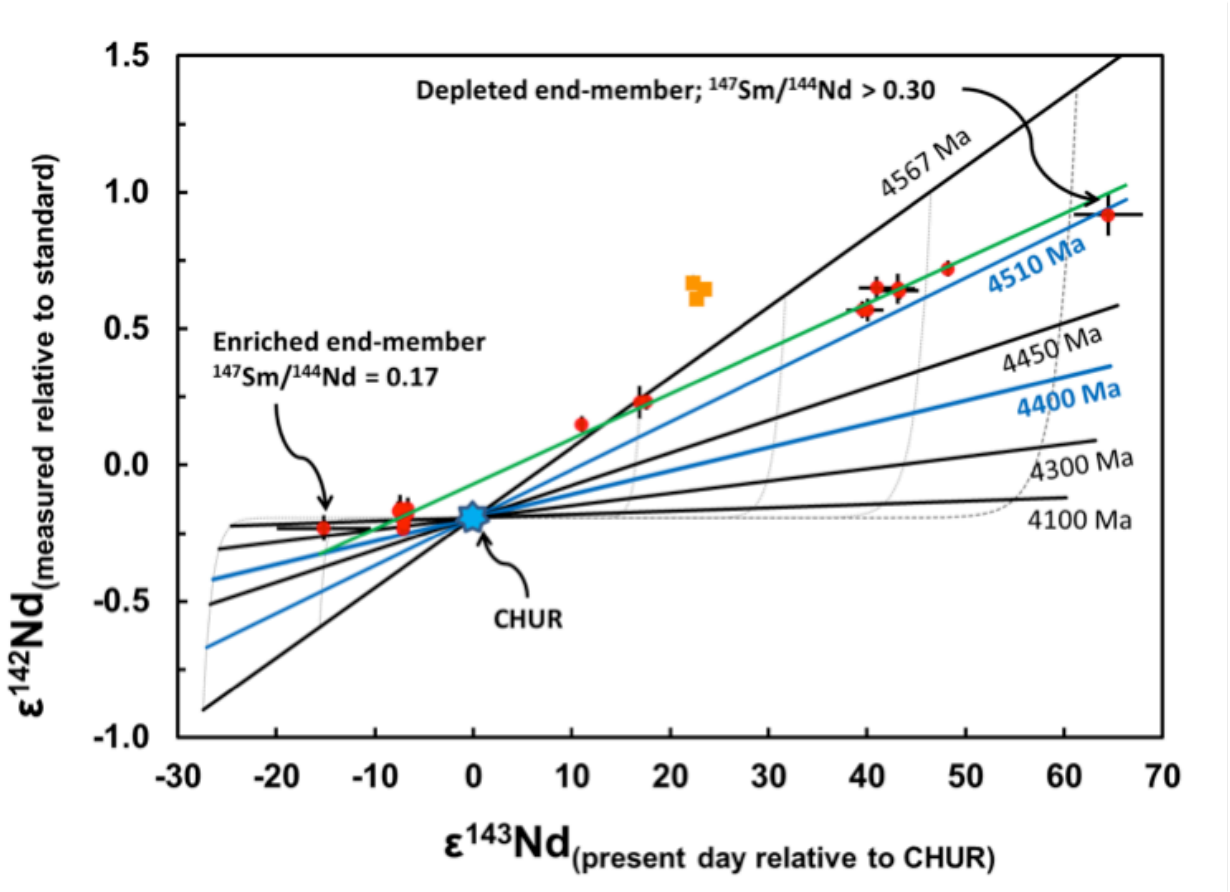

2140

2141 Figure 8

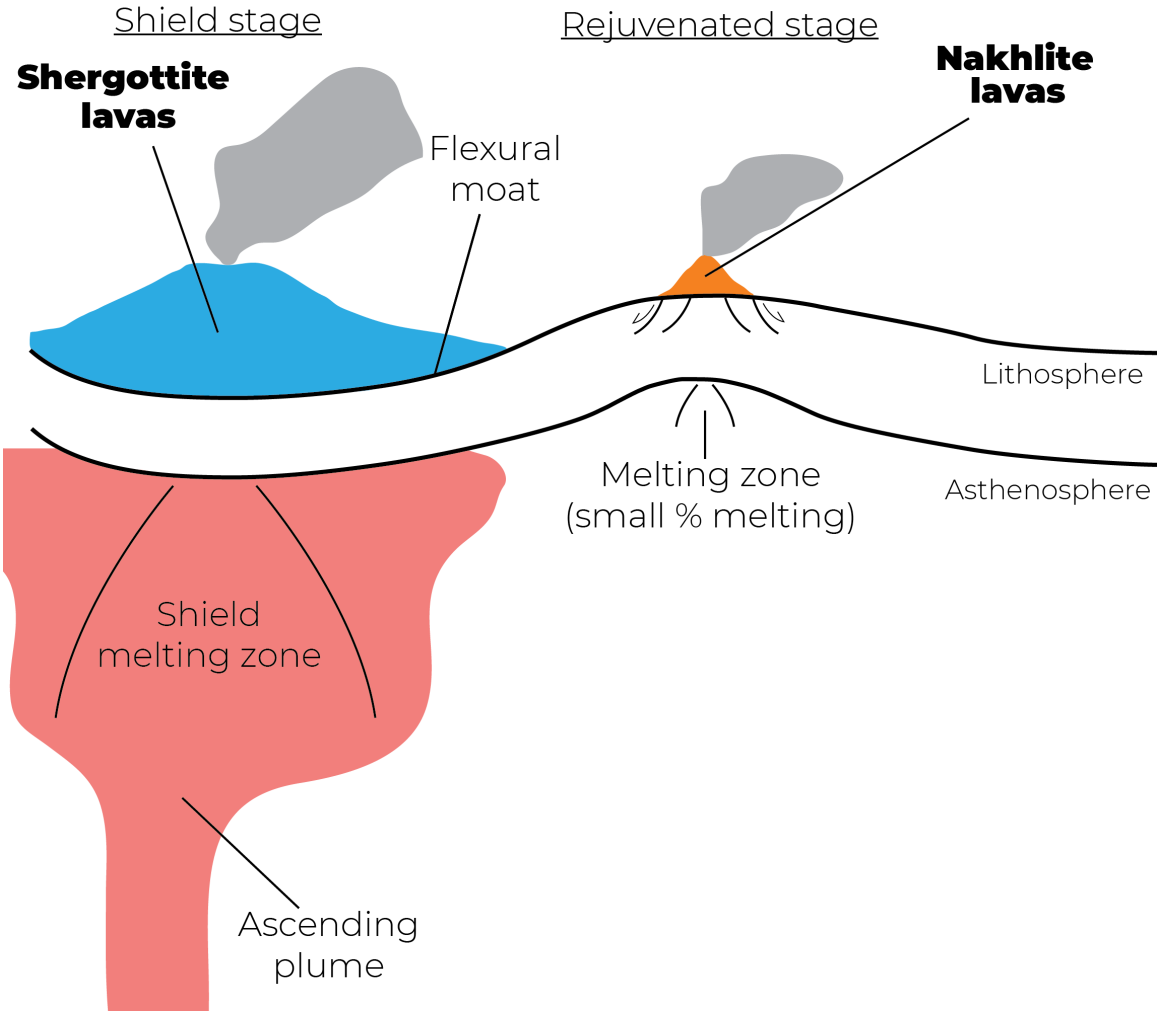

2142 Figure 9

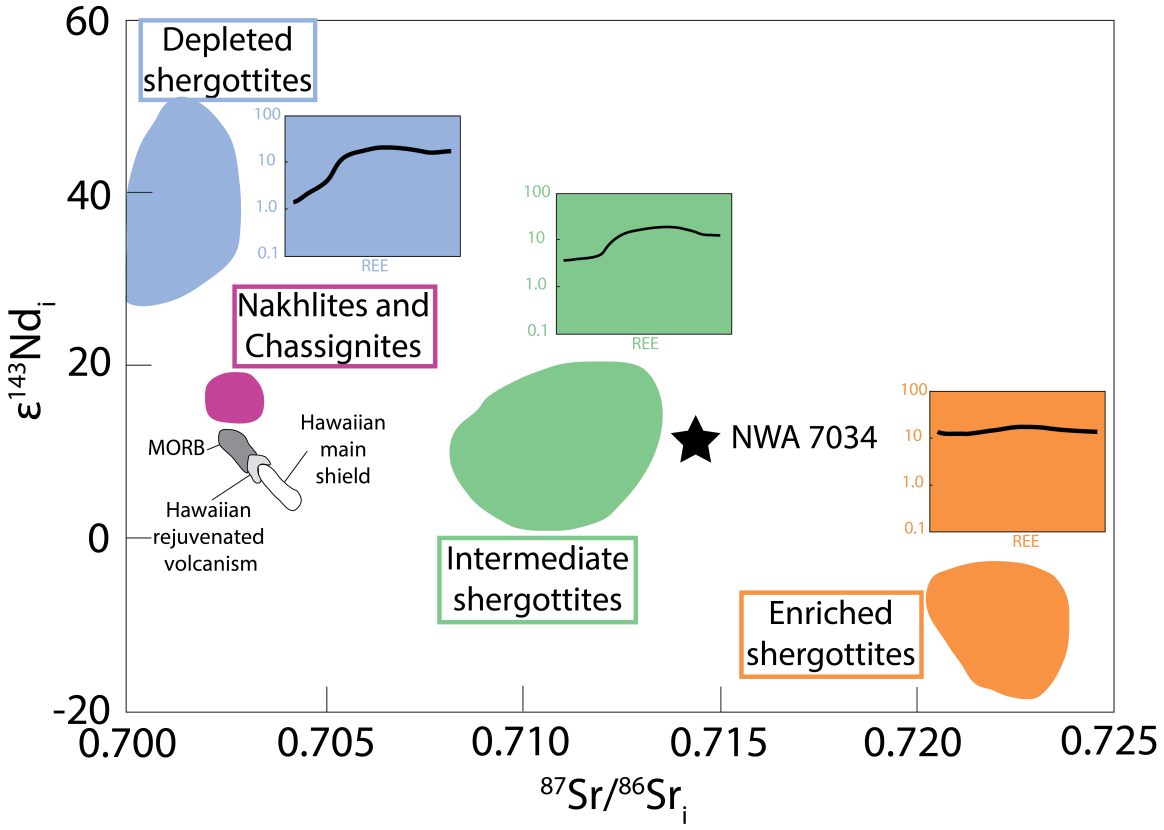

2143 Figure 10

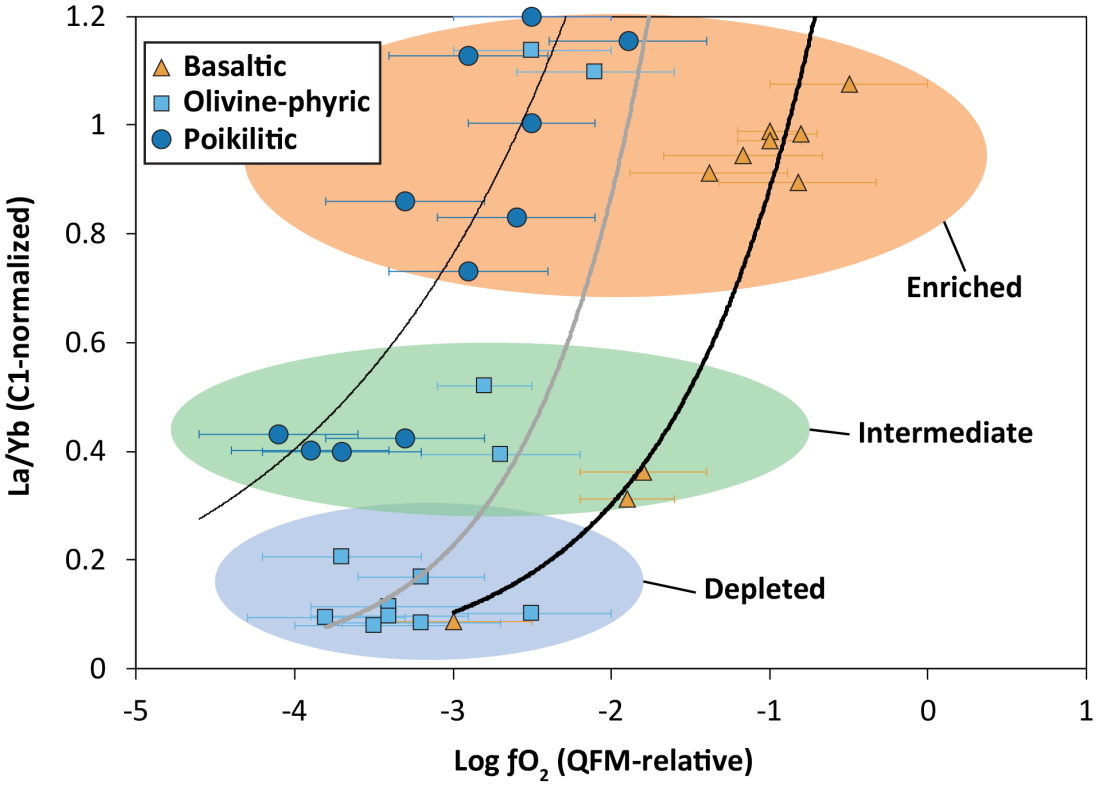

2144 Figure 11